GEOLOGICA CARPATHICA, DECEMBER 2019, 70, 6, 512–530 doi: 10.2478/geoca-2019-0030

Exhumation history of the Variscan suture: Constrains on the detrital zircon geochronology from Carboniferous–Permian sandstones (Northern Gemericum; Western Carpathians)

ANNA VOZÁROVÁ[1,✉], KATARÍNA ŠARINOVÁ[1], DUŠAN LAURINC[2], ELENA LEPEKHINA[3], JOZEF VOZÁR[4], NICKOLAY RODIONOV[3] and PAVEL LVOV[3]

[1]Comenius University in Bratislava, Faculty of Natural Sciences, Department of Mineralogy and Petrology, Mlynská dolina, Ilkovičova 6, 842 15 Bratislava, Slovakia; ✉anna.vozarova@uniba.sk, katarina.sarinova@uniba.sk
[2]State Geological Institute of Dionýz Štúr, Mlynská dolina 1, 817 04, Bratislva 11, Slovakia; dusan.laurinc@geology.sk
[3]Centre of Isotopic Research, A.P. Karpinsky Russian Geological Research Institute (FGBU «VSEGEI»), Sredny prospekt 74, 199 106 St.-Petersburg, Russia; Nickolay_Rodionov@vsegei.ru, Elena_Lepekhina@vsegei.ru, Pavel_Lvov@vsegei.ru
[4]Earth Science Institute of the Slovak Academy of Sciences, Dúbravská cesta 9, P.O. BOX 106, 840 05 Bratislava, Slovakia; jozef.vozar@savba.sk

(Manuscript received June 19, 2019; accepted in revised form October 25, 2019)

Abstract: The Late Paleozoic sedimentary basins in the Northern Gemericum evolved gradually in time and space within the collisional tectonic regime of the Western Carpathian Variscan orogenic belt. The detrital zircon age spectra, obtained from the Mississippian, Pennsylvanian and Permian metasediments, have distinctive age distribution patterns that reflect the tectonic setting of the host sediments. An expressive unimodal zircon distribution, with an age peak at 352 Ma, is shown by the basal Mississippian metasediments. These represent a relic of the convergent trench-slope sedimentary basin fill. In comparison, the Pennsylvanian detrital zircon populations display distinct multimodal distributions, with the main age peaks at 351, 450, 565 Ma and smaller peaks at ~2.0 and ~2.7 Ga. This is consistent with derivation of clastic detritus from the collisional suture into the foreland basin. Similarly, the Permian sedimentary formations exhibit the multimodal distribution of zircon ages, with main peaks at 300, 355 and 475 Ma. The main difference, in comparison with the Pennsylvanian detrital zircon assemblages, is the sporadic occurrence of the Kasimovian–Asselian (306–294 Ma), as well as the Artinskian–Kungurian (280–276 Ma) igneous zircons. The youngest magmatic zircon ages nearly correspond to the syn-sedimentary volcanic activity with the depositional age of the Permian host sediments and clearly indicate the extensional, rift-related setting.

Keywords: detrital zircon, U–Pb SHRIMP dating, provenance, tectonic setting.

Introduction

The kinematic evolution of the Western Carpathian orogenic system was created during both Variscan and Alpine orogeny. Fragments of newly formed Variscan crust were incorporated into the Alpine Western Carpathian units, which documents the repeating subduction/collision and transform fault processes. The Variscan crust was gradually amalgamated due to crustal thickening during Devonian/Mississippian collision events. The Tournaisian/Visean deep-water turbidite trough in the Northern Gemericum, originated in a convergent embayment and was continued as a Pennsylvanian peripheral basin. The Upper Pennsylvanian/Permian post-collisional evolution of the Western Carpathian realm continued by development of transtension/transpression and rift-related continental sedimentary basins.

Fragments of the Late Paleozoic sedimentary basin fillings are only preserved inside of the internal structural zone of the Alpine Western Carpathian orogeny. They became a part of the principal crustal-scale Alpine units of the Central and Inner Western Carpathians. These are arranged in an order from N to S and from bottom to top in the Tatricum, Veporicum, Northern and Southern Gemericum and several cover nappe systems (Fatricum, Hronicum, Bôrka Nappe as a part of Meliaticum, Turnaicum and Silicicum) (Biely et al. 1996a,b; Plašienka et al. 1997; Rakús et al. 1998; Plašienka 2018 and references therein).

Relics of the Carboniferous–Permian sedimentary sequences are present in the relatively wide range of sedimentary environments, evolving from deep-water through shallow-marine to paralic and continental. Within the framework of the whole Western Carpathian belt, the remnants of sedimentary rocks from this wide succession of sedimentary environments, and moreover in direct temporal sequence, are preserved only in the Northern Gemeric Unit (NGU; Fig. 1),. Petrofacial analysis of the Carboniferous–Permian sediments (Vozárová 1998 a,b), supplemented by the detrital zircon geochronology, directly reflects the process of tectono–thermal evolution and exhumation of the Variscan collision suture in the Western Carpathians. The U–Pb age dating of detrital zircons from this

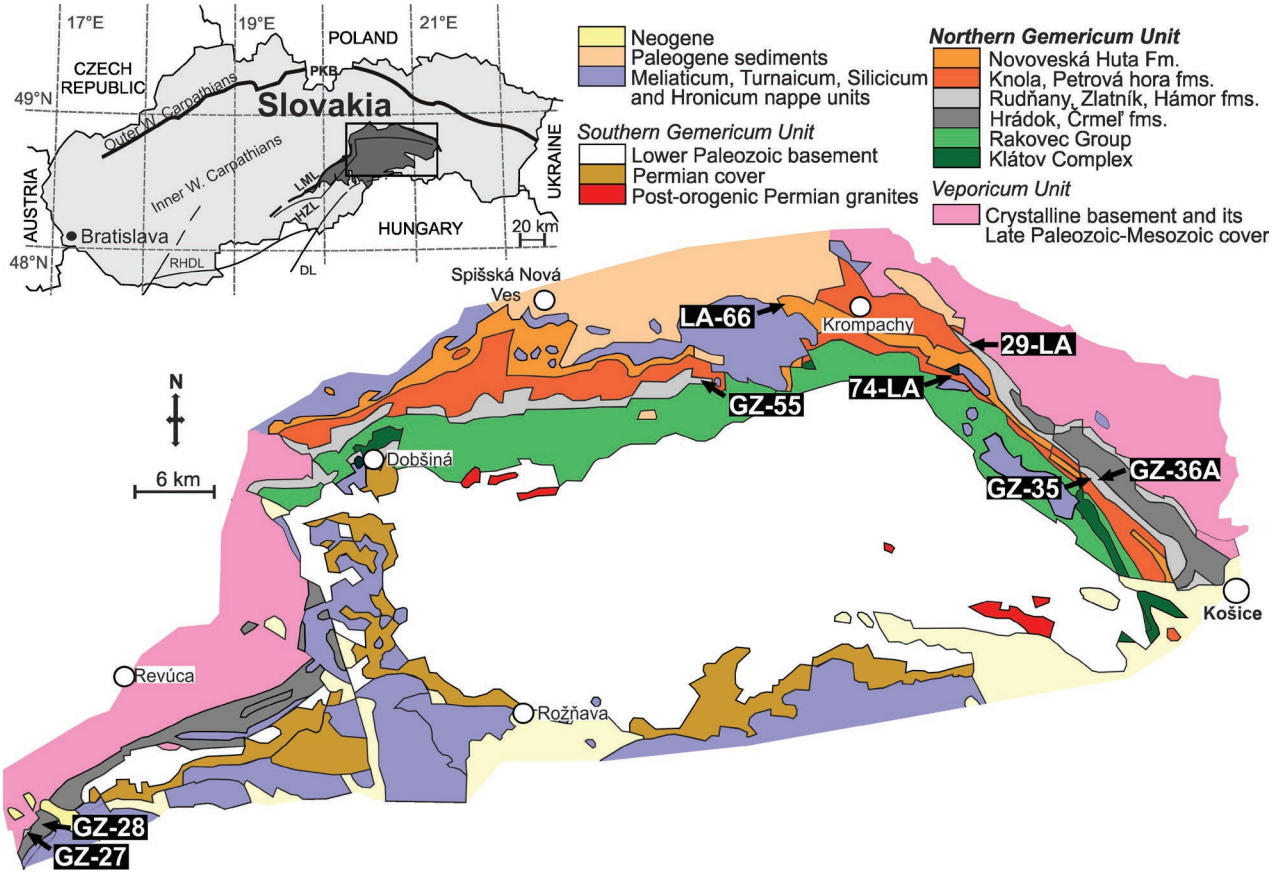

Fig. 1. Geological sketch of the Northern Gemericum (modified according to Biely et al. 1996 and Bajaník et al. 1984a), showing localities of the studied detrital zircon samples. *Abbreviations:* LML — Lubenik–Margecany Line; HZL — Hrádok–Železník Line.

area was completed for the first time by Vozárová et al. (2013). From the NGU Carboniferous–Permian sediments, 172 zircon ages were obtained, with a relatively wide age variance, ranging from 260 to 2700 Ma. Their mutual proportions were gradually changing, depending on the lithostratigraphy and time-scale, from the oldest to the youngest sediments. To this data set 126 new zircon data have been added with the intention of obtaining more detail background for interpretation.

Geological setting of the NGU Carboniferous–Permian sedimentary sequences

The NGU zone contains relics of the Variscan collision suture, characterized by thrust wedges of the two pre-Carboniferous terranes, the medium/high-grade gneiss–amphibolite Klátov Complex and the low-grade Rakovec Complex, and relics of the Mississippian syn-orogenic deep-water turbidite sequence. Pennsylvanian shallow-marine to paralic and Permian continental sedimentary basins postpone the main collisional events (e.g., Bajaník et al. 1983; Spišiak et al. 1985; Vozárová & Vozár 1988; Hovorka et al. 1988; Németh 2002; Németh et al. 2004; Ivan 2009; Radvanec et al. 2017). Deformational and metamorphic events recorded in both pre-Carboniferous terranes occurred in the Late Devonian–Mississippian, which is documented by their reworked rock fragments within the overstepping Pennsylvanian conglomerates (Krist 1954; Vozárová 1973, 2001) and by several geochronological data (Vozárová et al. 2005, 2013; Putiš et al. 2008, 2009a). Those terranes experienced Alpine reworking (Dallmeyer et al. 1996, 2005; Lexa et al. 2003; Vozárová et al. 2005, 2014; Putiš et al. 2009b).

Mississippian: The Mississippian formations have been preserved as tectonic relics at the W-SW and E-SE boundary of the NGU. These suffered a significant shortening as a result of Alpine thrusting of the NGU on the underlying Southern Veporicum in the footwall along the Lubeník–Margecany Line (LML; Andrusov 1959) (Fig. 1). Equally, the tectonic contact of the NGU with the Southern Gemericum is represented by the Hrádok–Železník Line (HZL) in the hanging wall (defined by Abonyi 1971), which continues into a system of thrust faults to the east (Fig. 1). The Mississippian turbidite wedges, supposedly derived from the Variscan suture, were interpreted as the fill of an intrasuture remnant ocean basin (Vozárová & Vozár 1988) or foredeep basin (Neubauer & Vozárová 1990; Ebner et al. 2008). In spite of orogenic/metamorphic reduction the present thickness of the Mississippian formations is estimated >1000 m (Vozárová 1996). A completely different opinion on the genesis of the Mississippian rock sequence was given by Novotná et al. (2015). The authors interpreted

the basal part of the Ochtiná Group (the Hrádok Fm. according to the lithostratigraphic classification by Vozárová 1996, Fig. 2) as a tectonic melange formed during the Cretaceous collision at the boundary of two major crustal nappes, the Gemericum and Veporicum. It is, however, necessary to emphasize that the Mississippian succession represents a sedimentary formation with typical features of deep-water turbidite sedimentation, but certainly strongly tectonically reworked during the Cretaceous orogenic processes.

The whole Mississippian sequence was deformed in the P–T conditions of greenschist facies. Fine-grained muscovite from the Hrádok Formation reflects the complex Alpine overprint

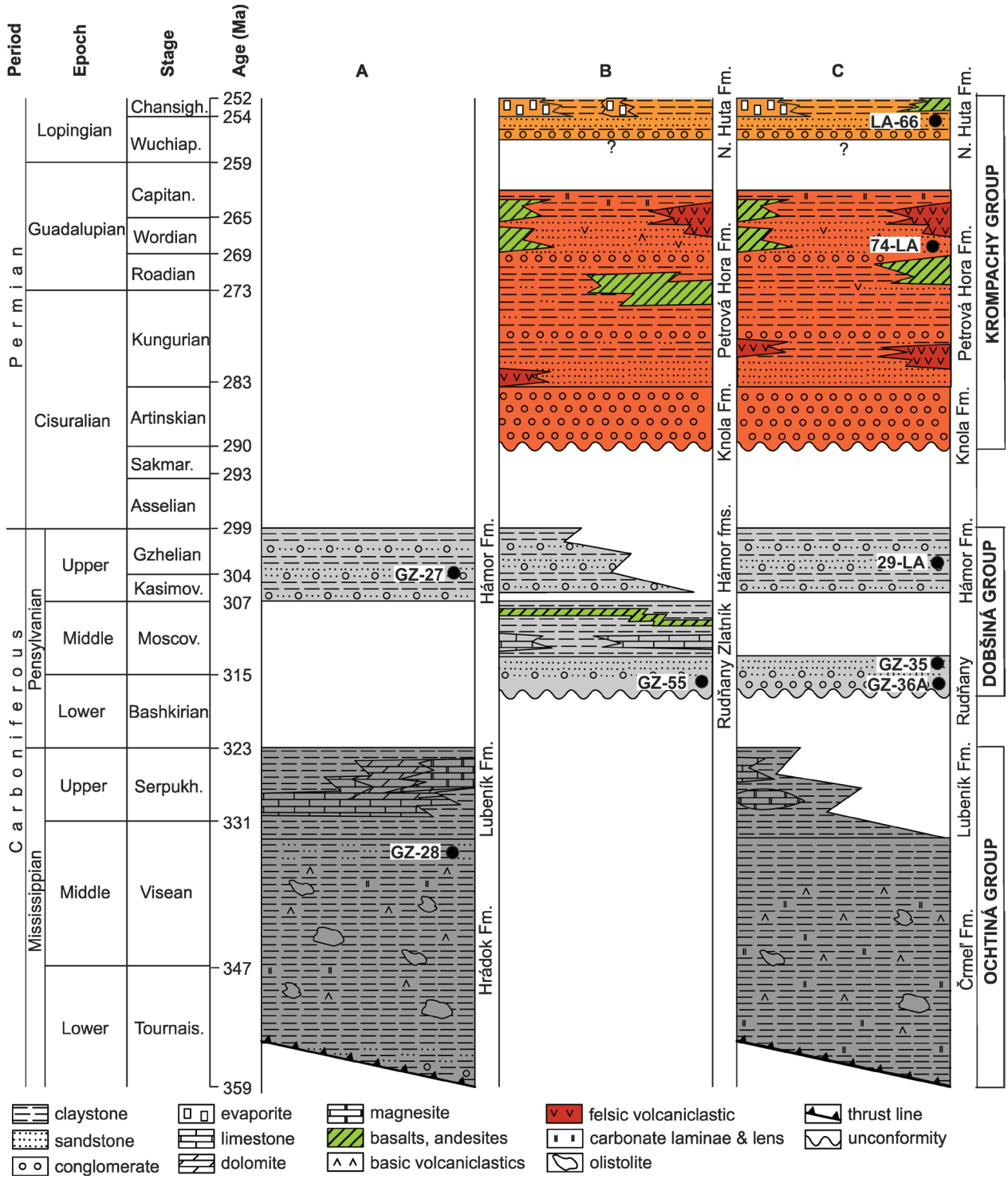

Fig. 2. Schematic lithostratigraphic columns of the Carboniferous–Permian sedimentary formations in the Northern Gemericum (modified after Bajaník et al. 1981; Vozárová 1996 and Vozárová et al. 2015) with sample locations. **a** — W and SW part; **b** — N part; **c** — E and SE part.

($^{40}Ar/^{39}Ar$ — 87 Ma at the rim to 142 Ma in the core, Vozárová et al. 2005; $^{40}Ar/^{39}Ar$ — 84 Ma, Putiš et al. 2009b). The Mississippian volcano-sedimentary sequence, defined by Vozárová (1996) as the Ochtiná Group (Fig. 2), is represented by the deep-water turbidite sediments in its lower part (the Hrádok and Črmeľ formations) and shallow-water, shaly-carbonate sediments in its upper part (Lubeník Formation, inclusive Bankov Beds).

The Hrádok Formation (Fm.) consists of a dark-grey and black clastic turbidite sequence, metaparaconglomerates, metasandstones, and metapelites, interlayered with metabasalts, metamicrodolerites and basic metavolcaniclastics. Sporadic lydites and siliceous metapelites were found only in thin layers and lenses. Slabs of ultramafic rocks (oceanic crust fragments) represented by antigorite serpentinites and tremolite-talc schists and scarce amphibolites as well as actinolite green-schists are integral part of this deep-water turbidite slope/rise sequence. A monotonous complex of dark-grey and black metapelites, overlying the relatively coarser-grained basal part of the Hrádok Fm., yielded a microflora indicating the Upper Turnaisian–Visean age (Bajaník & Planderová 1985).

The Mississippian sequence of the Črmeľ Fm. (Fig. 2c) represents a distal turbidite complex consisting of alternating metapelites, fine-grained metasandstones, basic to intermediate metavolcanics and its metavolcaniclastics, subsidiary carbonates and lydites (Bajaník et al. 1984a; Grecula 1998). Small amounts of acid volcanoclastic detritus are unevenly dispersed in its basal part. The Tournaisian–Visean age of the Črmeľ Fm. was indicated by microflora assemblages by Snopková in Bajaník et al. (1984b).

The overall upward-shallowing Mississippian sequence is interpreted as a reflection of progressive basin filling. The youngest Mississippian sedimentary rocks (Lubeník Fm.; Vozárová 1996; Fig. 2) are represented by the Upper Visean–Serpukhovian black shales and bioclastic carbonates, well documented by fauna, mainly in the western part of their occurrences (Bouček & Přibyl 1960; Kozur et al. 1976; Zágoršek & Macko 1994; Mamet & Mišík 2003).

Pennsylvanian: The Pennsylvanian transgressive sequence rests unconformably on the two NGU pre-Carboniferous complexes (Klátov and Rakovec) and, also, on the Mississippian succession in the E-SE realm of NGU (Fig. 2) and fix up the Variscan thrust/nappe structure. The Upper Bashkirian–Moscovian sequence started after a break of sedimentation, with boulder to coarse-grained delta-fan conglomerates (the Rudňany Fm., Fig. 2). They contain a detritus derived from both pre-Carboniferous complexes (Klátov and Rakovec), as well as, from the Mississippian sedimentary rocks (Krist 1954; Vozárová 1973; Vozárová & Vozár 1988). However, sporadic "exotic rocks", which do not occur on the NGU surface today, were found. They include pebbles of plagiogranites, granitoides, orthogneisses and metaquartzites (Vozárová 1973, 2001). Black shales and mica-rich grey sandstone intercalations are normal members of the fining upward Rudňany Fm. They contain Pennsylvanian macroflora remains which were determined by Němejc (1947). The 370—380 Ma $^{40}Ar/^{39}Ar$ cooling age data of white mica from metasandstones and gneiss pebble indicate a first step of the Variscan collisional suturing in the NGU zone (Vozárová et al. 2005). After initial rapid sedimentation the littoral to shallow-neritic limestones were associated with grey and black shales. This siliciclastic–carbonate lithofacies correspond to the basal part of the Zlatník Fm., which the Moscovian age is indicated by rich trilobite (Rakusz 1932; Bouček & Přibyl 1960) and conodont fauna (Kozur & Mock 1977).

The upper part of the Zlatník Fm. comprises fine-grained clastic metasediments associated with basalts and their volcaniclastics. Poor microfloral assemblages proved the Pennsylvanian age, but not an accurate division. This succession was formerly defined as the Zlatník Fm. (ZF) by Bajaník et al. (1981). However, Ivan (1997) and Ivan & Méres (2012) separated this complex of basic metavolcanics and metavolcaniclastics, associated with small amounts of fine-grained metasediments from the ZF. The authors defined this new lithostratigraphic unit as the Zlatník Group. This strongly contradicts the priority rule of the stratigraphic code (Michalík et al. 2007). If we assume that this set of basic volcanic lies in the tectonic position on the basal sediments of the ZF strata, then it should be included in the pre-Carboniferous NGU basement, most likely in the Rakovec Complex. This would also be indicated by the detected zircon ages from the ZF basic metavolcaniclastic, aged from 478 to 521 Ma (only four zircon grains, Vozárová unpublished data), as well as 388–382 Ma magmatic age from metabasalts (Putiš et al. 2009a). However, such a low number of zircon data does not entitle us to consider such an interpretation.

Termination of the Pennsylvanian peripheral basin is reflected by the paralic sequence of the Hámor Fm. (Fig. 2). It is characterized by distinct cyclical coarsening-upward shaly–sandy–conglomeratic sediments, an absence of synsedimentary volcanism and a local occurrence of ribbed coal seam. Poor microflora assemblages proved uppermost Moscovian age (Planderová & Vozárová 1980).

Permian: Continental Permian red-beds unconformably overlapped slightly deformed relics of the Moscovian peripheral basin filling, as well as two pre-Carboniferous NGU crystalline complexes and the Mississippian sequences (Fig. 2). Prevalent clastic sediments derived from the collision belt are associated with andesite/basalt–rhyolite volcanism (Rojkovič & Vozár 1972; Václav & Vozárová 1978; Bajaník et al. 1981, 1983; Novotný & Miháľ 1987; Rojkovič & Miháľ 1991 and references therein). The basal part (Knola Fm.) contains mostly poorly sorted polymictic conglomerates and breccias of extremely variable thickness, with pebble material reflecting the composition of the direct underlier (fossil mudflows relieved by alluvial, mainly stream channels, Vozárová 1996, 1998b). The polyphase volcanic activity manifested large sedimentary cycles. Sediments are characterized by a low degree of maturity and mixture of volcanic and non-volcanic detritus. The most striking features are the fining-upward alluvial cycles, with channel lag, point-bar and floodplain facies, alternating with playa at the topmost part of the large cycles.

The existing monazite and U–Pb SHRIMP zircon ages yield Cisuralian ages (Kungurian) for both, the acid and basic volcanic members (278 Ma — monazite, Rojkovič & Konečný 2005; 272–275 Ma — U–Pb zircon ages, Vozárová et al. 2012). The last volcanic phase was linked with extension at the Permian–Triassic boundary, connected with the beginning of the Alpine orogenic cycle (257.2±3.0 and 255.6±3.7 Ma Re–Os molybdenite ages, Kohút et al. 2013; 251±4 Ma U–Pb zircon ages, Vozárová et al. 2015).

The NGU Permian–Triassic volcanic event seems to be approximately coeval with the sedimentation of the Novoveská Huta Fm. evaporite member that is correlated with the Zechstein (Continental Stage) based on S and O isotopes (Kantor et al. in Vozárová 1997). The polymictic conglomerates (the Strážany Beds; Mihál' in Rojkovič & Mihál' 1991) that underlie this evaporate lithofacies, contain fragments of volcanics, which were redeposited from the Cisuralian volcanic suite. On the account of that, the stratigraphic gap from the mid-Guadalupian to the Lopingian, is supposed to be trustworthy (Vozárová et al. 2015) (Fig. 2c).

Analytical methods

The rock-forming minerals were studied by an electron microprobe (CAMECA SX-100, in the laboratory of the Geological Survey of Slovak Republic, Bratislava). Zircons have been extracted from the rocks by standard grinding, heavy liquid and magnetic separation analytical techniques. The internal structure of individual zircon crystals was examined with cathodoluminescence (CL) imaging by SEM (CamScan M2500 Oxford Instruments). In situ U–Pb analyses were performed using a Sensitive High-Resolution Ion Microprobe (SHRIMP-II) at the Centre of Isotopic Research (CIR) in A.P. Karpinsky Russian Geological Institute (VSEGEI), by applying a secondary electron multiplier in peak-jumping mode, based on the procedure described by Williams (1998). Primary beam size allowed for the analysis an area of ca. 25×20 μm. CL, BSE and optical (transmitted light) imaging was applied to reveal the internal and surface features that were used to choose the position of analytical spots on the mostly homogeneous inclusion-free parts of individual zircon grains. The 80 μm wide ion source slit, in combination with a 100 μm multiplier slit, allowed for the mass-resolution $M/\Delta M \geq 5000$ (1% valley); hence, all the possible isobaric interferences were resolved. The following ion species were measured in the sequence: $^{196}(Zr_2O)$–^{204}Pb–background (ca. $^{204.5}$AMU)–^{206}Pb–^{207}Pb–^{208}Pb–^{238}U–^{248}ThO–^{254}UO. At least 4 mass-spectrums were acquired for each analysis. Zircon Temora-1 (Black et al. 2003) was measured as the main reference material (RM): one analysis per every four analyses of unknowns to obtain their U/Pb ratios. Zircon 91500 (Wiedenbeck et al. 1995) was used as a concentration RM. The obtained results were processed by the SQUID v1.12 (Ludwig 2005) and ISOPLOT/Ex 3.75 (Ludwig 2012) software, with decay constants recommended by Steiger & Jäger (1977), including modern corrections, e.g. Hiess et.al (2012). Common lead correction was done on the basis of the measured ^{204}Pb/^{206}Pb ratio. The ages given in this text, if not additionally specified, are ^{207}Pb/^{206}Pb for zircon older than 1.0 Ga, and ^{206}Pb/^{238}U for those younger than 1.0 Ga. The degree of discordance was calculated according to the following formula: $\%\ D = 100 * (Age^{207/206}/Age^{206/238} - 1)$. The uncertainties are quoted at standard deviation level (1s, i.e. 68.3 % confidence) for individual points and at 2 s level in the Concordia diagram, for the Concordia ages or any previously published ages discussed in the text. Age distributions of detrital zircons are displayed as Kernel Density Estimates (Vermeesch 2012). Only analyses that produced concordant ages within 10 % ($-10 < \%\ D < +10$) were used. The time-scale calibration of the International Chronostratigraphic Chart (2018-8) was used to compare geochronological data from detrital zircons with fossil-bearing sedimentary units and tectono–thermal events.

Results

Sample characteristics

Seven samples have been processed for zircon dating from the Carboniferous–Permian sandstones of the NGU succession (Figs. 1, 2). From one previously dated sample an additional zircon dating was made (***LA-66***; Vozárová et al. 2013).

Hrádok Fm.: The sample ***GZ-28*** was collected from the upper part of the Hrádok Fm., SE from the Sušanský vrch elevation, along a forest road cut, 421 m above sea level (GPS coordinates: 48°35.504'N, 20°03.076'E). This metasandstone displays a strong foliation, with indication of crenulation cleavage in places. Primary mineral composition was considerably changed due to a strong Alpine deformation and recrystallization. Quartz and detrital micas are the most frequently preserved detrital grains. Primary clayey matrix and feldspar clasts were recrystallized and became a fine-grained aggregate of "pseudomatrix" (ca. 40 % of the whole rock). This consists of quartz+muscovite±paragonite and graphite.

Rudňany Fm.: Two cobbles from the basal part of the Rudňany Fm. were gathered for zircon dating. The sample ***GZ-36A*** was collected from the forest slope cliff east of the Košická Belá Village, 478 m above sea level (GPS coordinates: 48°48.443'N, 21°07.083'E). This is represented by the metaquartzite with non-uniform granoblastic texture and relics of primary roundness on the surface of selected quartz grains. Besides quartz grains (ca. 98 %) scarce fragments of acid felsites and quartzose phyllites were recognized. Zircon, rutile and tourmaline are common heavy minerals.

The cobble ***GZ-55*** was taken from the forest cliff SE of the Poráč Village, 650 m above sea level (GPS coordinates: 48°52.220'N, 20°42.531'E). It represents biotite–plagioclase orthogneiss with a lepidogranoblastic texture that is characterized by alternating light and dark bands differing in mineral composition. The light bands contain mainly quartz and plagioclase and only sporadic orthoclase. Plagioclases express

an oligoclase composition range (Or=1 %, Ab=75 %, An=24 %; average from five analysis) (Supplement, Table S1). K-feldspar is perthitic with microcline twinning in places. The darker bands consist of biotite associated with small amounts of garnet (Prp=9 %, Sps=5 %, Alm=71 %, Grs=15 %; average from three analyses). The minerals are oriented parallel to schistosity. This gneissic rock was affected by powerful secondary alteration, manifested by a sericitization of feldspars and a total chloritization of biotite and partially of garnet. Accessory apatite and zircon are present.

The sample ***GZ-35*** represents the composition of sandstones from the upper part of the Rudňany Fm. It was collected along the small gorge at the E edge of the Košická Belá Village, 413 m above sea level (GPS coordinates: 48°48.317'N, 21°06.913'E). This coarse-grained sandstone is strongly foliated, with individual greater clasts deformed along the foliation planes. Quartz, detrital micas and lithic fragments of different phyllites, mica schists and volcanics are the prevalent primary association. Feldspars are present sporadically. Recrystallized "pseudomatrix" is characterized by preferred orientation of quartz–sericite aggregates, which most probably also involved a part of the lithic fragment detritus.

Hámor Fm.: Two samples have been collected from the Hámor Fm. The sample ***GZ-27*** comes from western edge of the Poproč Village, 555 m above sea level (GPS coordinates: 48°35.082'N, 20°01.950'E). As a consequence of a strong Alpine deformation in the shear-zone along the LML (Fig. 1), the metasandstone is strongly recrystallized and foliated. The dominant part of the mineral composition is formed by undulatory quartz grains, which have undergone a dynamic recrystallization. Other immature detrital grains (supposed feldspars or volcanic and lithic fragments) are completely recrystallized into strongly preferred, fine-grained quartz+sericite±graphite aggregates. Detrital mica is distinguishable.

The sample ***29-LA*** was collected along a regional road cut 1 km SW from the Margecany Village, 343 m above sea level (GPS coordinates: 48°53.208'N, 21°00.339'E). Prevalent quartz grains (73 %), associated with plagioclase (7 %), K-feldspar (4 %), detrital mica (4 %) and lithic fragments (12 %) are characteristic for the mineral composition of this quarzolithic metasandstone. Various types of phyllites, fine-grained sandstone, lydite, acid volcanics and sporadically crystalline schists have been identified among the lithic fragments. The studied metasandstone is characterized by a massive, partly foliated blastopsammitic texture. Dominant are the clastic grains displaying a variable degree of pressure solution and a fine-grained recrystallized matrix (on average 20 %), consisting of quartz+sericite±chlorite, with preferred orientation.

Petrova Hora Fm.: The sample ***74-LA*** was taken from the eastern occurrences of the Petrova Hora Fm., 1.2 km W from the Jaklovce Village, 361 m above sea level (GPS coordinates: 48°52.131'N, 20°58.670'E). This sandstone displays red-violet colour and immature mineral and textural composition, typical for "red-beds" facies. Among detrital grains the quartz (55 %), plagioclase (8 %), K-feldspar (4 %), volcanic and lithic fragments (16 %) and detrital micas (17 %) were recognized. Relatively rich matrix (27 %) contains quartz, sericite and abundant hematite pigment.

Novoveská Huta Fm.: No new sample was collected from the Novoveská Huta Fm. The original sample ***LA-66***, published in the article Vozárová et al. (2013) has been supplemented by new 10 measurements that were once again recalculated together with the older age data.

Zircon dating

Mississippian population

The detrital zircon age data were acquired from the sample ***GZ-28***, which was collected from the upper part of the Hrádok Formation (Fig. 2). Comparison with the previously published sample ***LA-81*** (Vozárová et al. 2013), which was located in the basal part of the Hrádok Formation, established the occurrence of the Early Ordovician/Late Cambrian detrital zircon ages in the range from 482±5 to 509±6 Ma (Fig. 3). All of them show characteristic features of a magmatic origin, with the $^{232}Th/^{238}U$ ratio values between 0.29 and 0.39 and oscillation growth zoning (Fig. 3c; Supplement, Table S2). One exception is represented by spot 12, which gave the 499±4 Ma age (Fig. 4). That was indicated by the narrow rim that mantled the oscillatory zoned and corroded zircon core. The main characteristics of spot 12 are low $^{232}Th/^{238}U$ ratio value (0.09) and texture indicating a local recrystallization.

The second group of detrital zircons is determined by the Visean and Famennian ages. Two of them, 330±2 and 367±4 Ma old, show the typical features of magmatic origin with fine oscillation growth zoning and characteristic $^{232}Th/^{238}U$ ratios of 0.40 and 0.95, respectively. Two other zircon grains display the age of 340±2 and 368±2 and low $^{232}Th/^{238}U$ ratios of 0.02 and 0.04, respectively (Fig. 3c). Both zircons are preserved as the homogeneous inherited cores, which were mantled by the fine-oscillation growth zoned rims.

The last group of detrital zircon ages belongs to the Precambrian. One spot is 566±6 Ma old (Ediacaran) and other one 2045±27 Ma old (Orosirian). Further three zircon grains are ranging from 2694±13 to 2760±8 Ma (Neoarchean).

Thus, the studied detrital zircon age distribution, shown by the Probability Density Plot (PDP), identify the main peak at the 340, 483 Ma and further smaller peaks at 568 and 2696 Ma (Fig. 3b).

Pennsylvanian population

Rudňany Formation — basal part

The sample ***GZ-36A*** represents metaquartzite, indicating the detrital origin of the all analysed zircon grains. From the investigated detrital zircon set, Phanerozoic age was found in only one zircon grain, which corresponds to the 537±6 Ma (lowermost Cambrian, Fortunian Stage) (Supplement, Table S2). All others zircon data confirm the Precambrian with

dominance of the Paleoproterozoic, ranging from 1888±28 to 2136±13 Ma (7 grains) and the Neoarchean, ranging from 2514±24 to 2770±11 Ma (7 grains). The last two zircon grains gave the 2834±20 and 2941±22 Ma ages that document Mesoarchean. Correspondingly, the remarkable age peaks on the PDP are at 2028 and 2688 Ma age and smaller peaks at 537 and 576 Ma (Fig. 5). Evidently, the majority of the analysed zircon grains show a typical feature of magmatic origin, reflected by the $^{232}Th/^{238}U$ ratio values within the range of 0.27–1.95 (Fig. 3c). This is also documented by the fine growth oscillatory zonation. However, within the Paleozoic and Archean zircons later recrystallization can be observed, which has led to a gradual fading of original growth zoning. This could be correlated with Pb loss, probably caused by a later metamorphic recrystallization (Fig. 4). Among the studied detrital zircon assemblage only one grain 2007±18 Ma is characterized by a very low $^{232}Th/^{238}U$ ratio value (0.08) and homogeneous internal texture, suggesting thus a metamorphic origin (Fig. 3c; Supplement, Table S2).

The sample ***GZ-55***, represented by the orthogneiss cobble, displayed a further unique zircon population (Supplement, Table S2). The Concordia diagram clearly shows the bimodal distribution of the age data, corresponding to the Middle/Upper Devonian and Cambrian, respectively (Fig. 5). Cambrian ages, ranging from 510±1.5 to 534±2.5 Ma are dominant. The $^{206}Pb/^{238}U$ Concordia age, calculated from the three concordant spots, gave 508.8±4.3 Ma (Fig. 5). All of the analysed grains show the $^{323}Th/^{238}U$ ratio values in the range of 0.20–0.39, indicating origin from acid magmatic rocks (Fig. 3c). Relics of the fine oscillatory growth zoning is currently observed, with some traces of recrystallization (enclaves of convolute or patchy textures). A further two zircon grains produced younger ages, 504.4±1.6 Ma and 491.6±3.8, and are characterized by relatively lower $^{232}Th/^{238}U$ ratio values, 0.08 and 0.10, respectively (Fig. 3c). This strongly indicates a late magmatic or metamorphic recrystallization. It is necessary to emphasize that all studied zircon grains are mantled by the narrow light rims. Two of these rims, those that could be

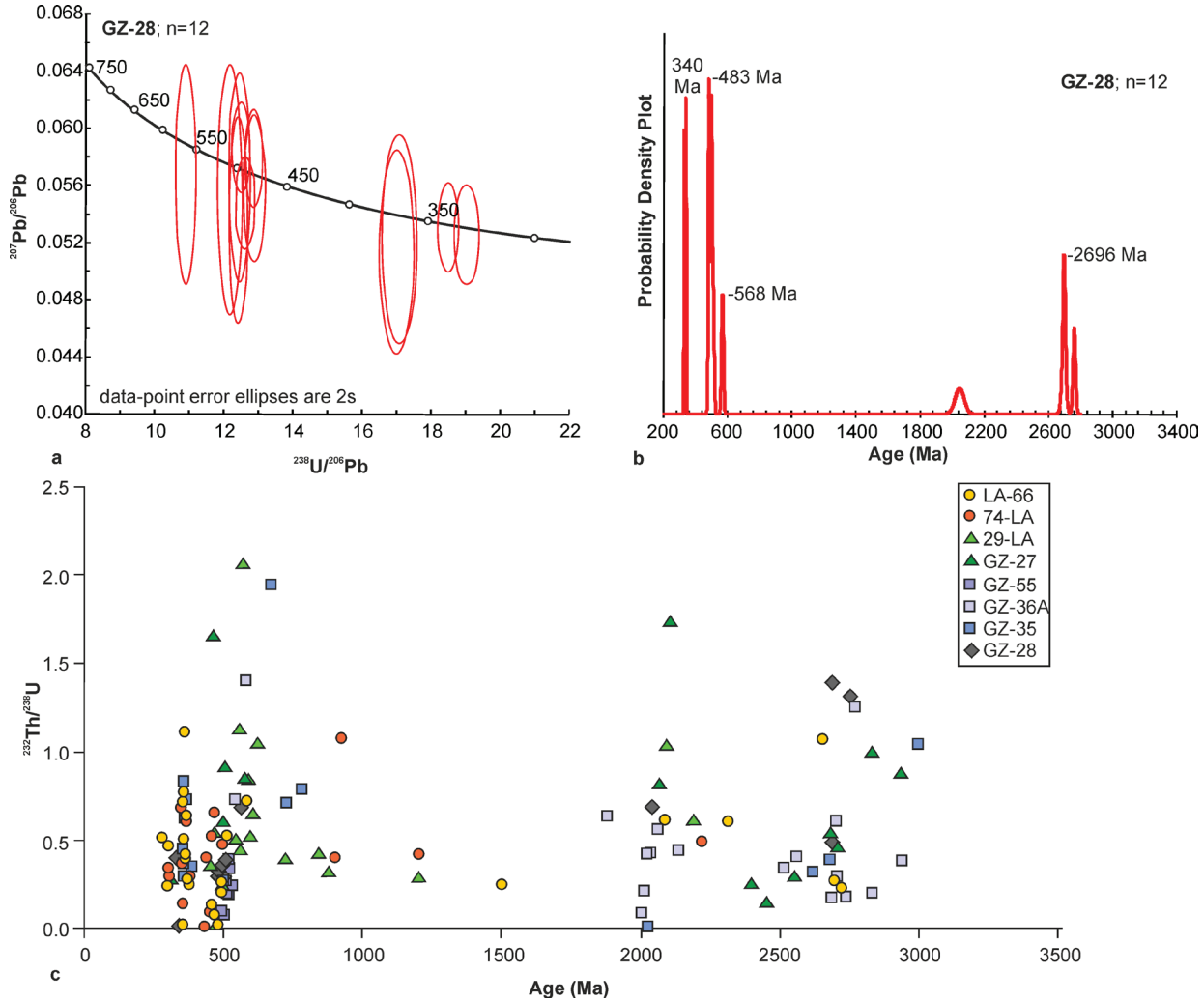

Fig. 3. a — Selected sector of the Concordia from the sample *GZ-28* (Hrádok Fm.) relevant to the most prominent cluster for age spectrum from 750 to 350 Ma. **b** — Corresponding PDP of detrital zircon ages. **c** — Th/U ratios of detrital zircons from the NGU Carboniferous–Permian metasediments vs. time scale.

Fig. 4. Selected CL images of detrital zircons from the studied samples.

measured, were analysed and gave ages of 385.7±6.3 and 386.7±4.9 Ma that are almost equal within the error (Fig. 4). The relatively low $^{232}Th/^{238}U$ ratio values, 0.06 and 0.01, respectively, indicate metamorphic recrystallization.

Rudňany Formation — upper part

This is represented by a detrital zircon population from the sandstone samples ***GZ-35***. The comparable detrital zircon

groups are represented by the Tournaisian–Famennian ages, ranging from 350.8±5.2 to 363.9±5.4 Ma. The $^{206}Pb/^{238}U$ Concordia age, calculated from the six concordant spots, gave 355.9±4.3 Ma, which is well indicated by 356 Ma peak on the PDP diagram (Fig. 6). The $^{232}Th/^{238}U$ ratios of less than 1, ranging between 0.30 and 0.84, as well as a growth zoning indicate their derivation from an acid magmatic source (Fig. 3c). The older Phanerozoic detrital zircons are 384.1±5.5 and 497.1±7.7 aged, with $^{232}Th/^{238}U$ ratio values of 0.35 and 0.27, respectively (Supplement, Table S2).

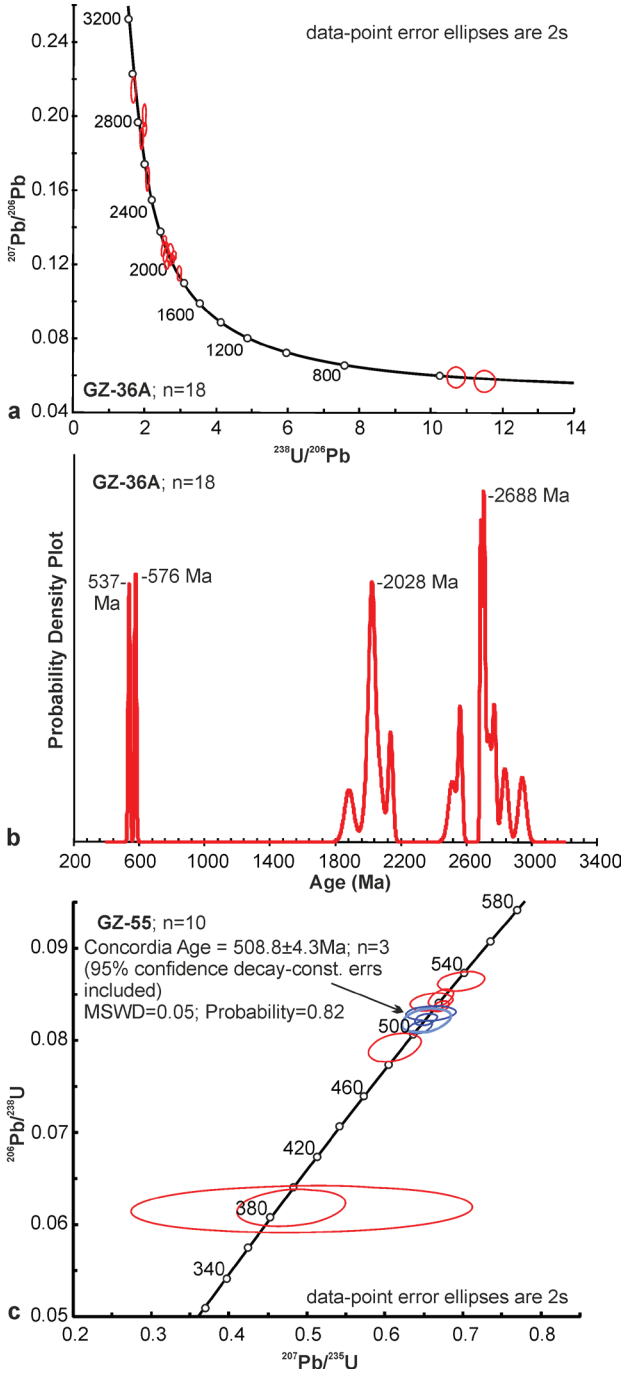

Fig. 5. a — Concordia plot of zircons from the Rudňany Fm. metaquartzite cobble (*GZ-36A*). **b** — Corresponding PDP. **c** — Concordia plot of zircons from the Rudňany Fm. gneiss cobble (*GZ-55*), with indication of the Concordia age.

Next part of the ***GZ-35*** detrital zircon set is formed by the Precambrian population. From those two zircon grains yielded Cryogenian, 671.7±9.7 and 724.0±12 ages. The other grain gave 781.0±13 Ma of Tonian age. Among these, only 671.7 Ma zircon exhibits the $^{232}Th/^{238}U$ ratio higher than 1 (1.95), what reveals a basic magmatic source (Fig. 3c). A further five zircon grains belong to the Mesoproterozoic (2028.0±8 Ma), the Neoarchean (2619.5±8.3 and 2665.7±9.7 Ma) and the Mesoarchean (2998.0±16 Ma). Based on the $^{232}Th/^{238}U$ ratios, the majority of these zircons demonstrate acid magmatic sources. The only exception is the zircon grain 2028 Ma old with 0.01 $^{232}Th/^{238}U$ ratio value, presumably indicating a metamorphic source (Supplement, Table S2).

Thus, the whole Rudňany Fm. zircon assemblage (samples *GZ-35+GZ-36A+GZ-55*) indicate the following four age peaks on the PDP diagram: 356, 518, 2028 and 2688 Ma (Fig. 6.).

Hámor Formation

Two samples have been collected from the Hámor Formation; sample ***29-LA*** from the eastern and sample ***GZ-27*** from the western part of the NGU surface occurrences (Figs. 1, 2).

Sample ***29-LA***: The youngest detrital zircon ages vary from 346.2±5.8 to 383.0±6.3 Ma (Fig. 7). Fine oscillation growth zoning, as well as $^{232}Th/^{238}U$ ratio values between 0.29 and 0.38 indicate derivation from an acid magmatic source (Fig. 3c; Supplement, Table S2). The Middle Ordovician magmatic source is documented by two grains, 464.7±7.5 and 453.0±7.6 Ma old ($^{232}Th/^{238}U$ ratios 0.36 and 055). Besides, the 475.7±8 Ma homogeneous metamorphic rim ($^{232}Th/^{238}U$ ratio=0.02), the mantled old core 1269.0±7.1 was observed (Supplement, Table S2). One solitary detrital zircon grain of 496.8±8.1 (Furongian) was found. A frequent set of detrital zircons ranges from 544.7±8.8 Ma to 622.0±14 Ma. The Concordia age, calculated from seven concordant data yielded 595.0±12 Ma, which clearly represents the Ediacaran Period. Three further zircon grains in the age of 724.0±13, 843.0±17 and 878.0±14 Ma correspond to the Tonian. The oldest zircons detected are 2095.0±13 and 2195.0±10 Ma old. In general, the distribution of detrital zircons ages is well presented on the PDP with the main peaks at 468, 561 and 596 Ma and small peak at ~2.1 Ga (Fig. 7).

The majority of the studied detrital zircons demonstrate the $^{232}Th/^{238}U$ ratio values less than 1, thus indicating acid magmatic sources (Fig. 3c). Some Ediacaran zircons show $^{232}Th/^{238}U$ ratio values in the range of 1.04–2.07, which could specify an intermediate and/or mafic magmatic source (Supplement, Table S2).

Sample ***GZ-27***: Compared to the sample ***29-LA***, the age spectrum of detrital zircons begins at the Moscovian, which is denoted by the two grains of 308±2 and 309±2 Ma old (Fig. 7). Both display by their oscillatory growth zoning and $^{232}Th/^{238}U$ ratio values of 0.85 and 0.28, respectively. One zircon grain

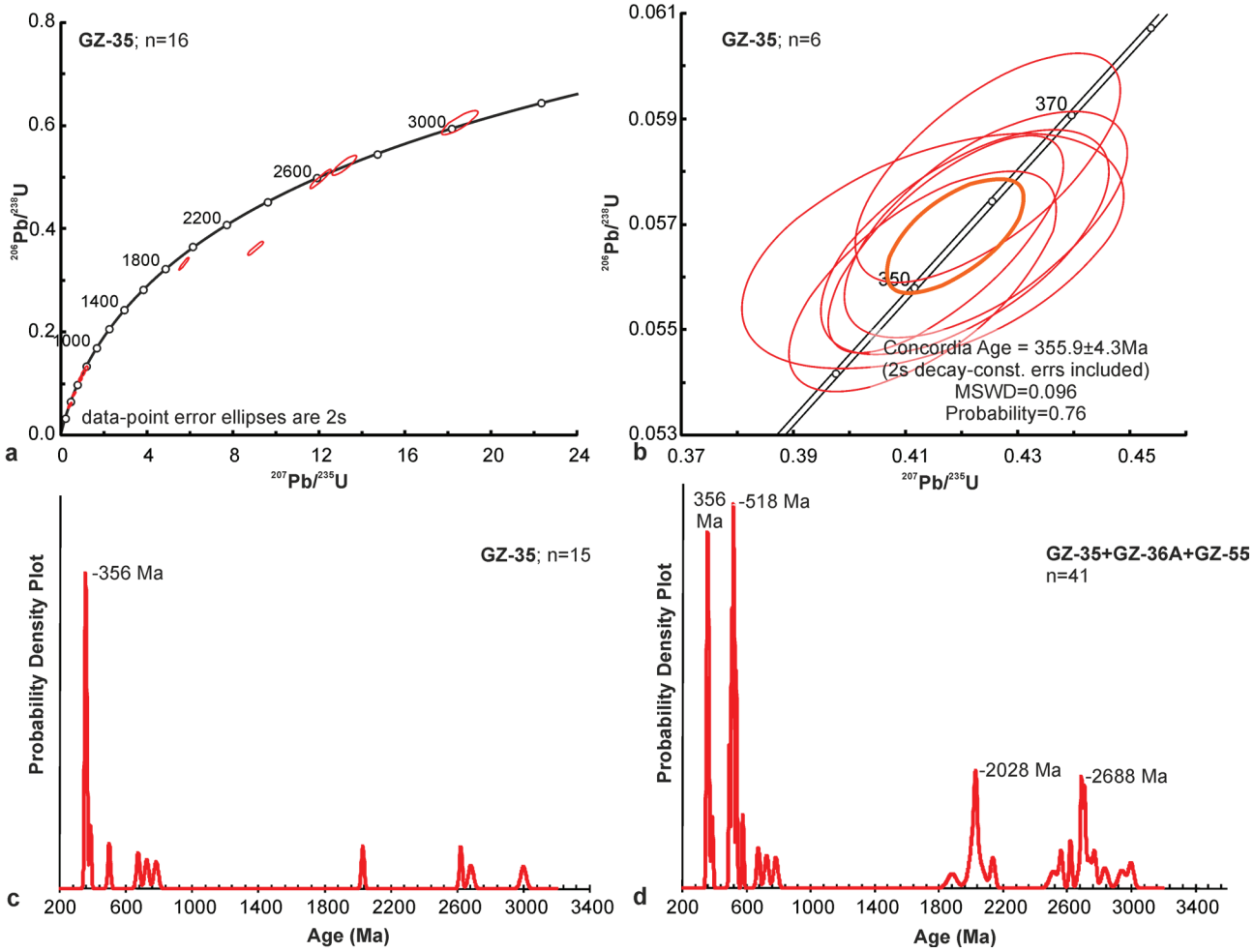

Fig. 6. Concordia plot of detrital zircons from the upper part of the Rudňany Fm. (*GZ-35*). **a** — all detrital zircon ages. **b** — Selected sector for age spectrum from 340 to 380 Ma, showing the Concordia age of prominent detrital zircon population. **c** — Corresponding PDP. **d** — PDP diagram for the all dated zircons from the Rudňany Fm. (*GZ-35, GZ-36A, GZ-55*).

revealed the 460±5 Ma age (Middle Ordovician), characterized by growth zoning and a relatively high $^{232}Th/^{238}U$ ratio value, equalling to 1.66 (Fig. 3c). The next group of zircons is signified by three Cambrian grains, aged from 497±4 to 522±9 Ma. All display the growth zoned internal texture and $^{232}Th/^{238}U$ ratio values in the range of 0.61–1.22, which indicate derivation from an acid/intermediate magmatic source (Fig. 3c; Supplement, Table S2). The whole age spectrum of detrital zircon ages is clearly visible on the PDP, especially the peaks at 309 and 502 Ma, and two sub-peaks at 578 and 2450 Ma (Fig. 7).

More than half the studied detrital zircon grains proved Precambrian ages (Supplement, Table S1). From these, one grain is identical with Ediacaran, of the 577±6 Ma aged. A further nine zircon grains are scattered from 2066 to 2936 Ma. Three of them express the Paleoproterozoic, ranging from 2066±38 to 2451±13 Ma and additional two Neoarchean of 2552±15 and 2681±15 Ma. The oldest group of detrital zircons belong to the Mesoarchean with ages of 2709±15, 2832±26 and 2936±13 Ma (Supplement, Table S1).

Permian population

Petrova Hora Formation

The cluster of detrital zircon data from the sample ***74-LA*** yielded concordant ages, mainly between 298 and 493 Ma (Fig. 8; Supplement, Table S2). The youngest detrital zircon gave the age of 298.4±5.7 and 303.4±6.8 Ma, both almost within the analytical errors. They display a fine-oscillation growth zoning and 0.34 and 0.30 $^{232}Th/^{238}U$ ratio values, compatible with an acid magmatic source (Fig. 3c). The 300.8±8.1 Ma Concordia age has been provided from these two data. However, among the studied detrital zircon set, Late Devonian–Mississippian ages, ranging from 346.4±6.6 to 379.4±7.2 Ma are prevalent, with $^{232}Th/^{238}U$ ratios from 0.14 to 0.69. The Concordia age, calculated from four concordant spots, gave 353.4±6.5 Ma (Fig. 8). Rare Silurian ages were determined for two grains. The first grain documents a magmatic event at 434±8 Ma with $^{232}Th/^{238}U$ ratio value of 0.40. The second grain corresponds to the 433±9 Ma of the Middle

Silurian metamorphic event and has a characteristic low $^{232}Th/^{238}U$ ratio value (=0.01). Three detrital zircon grains gave the Middle-Upper Ordovician age, whereas one grain presented age of 448.9±8.4 Ma with a relatively low $^{232}Th/^{238}U$ ratio value (=0.09). Nevertheless, this grain shows a growth zoning even in internal texture, though slightly deformed. The other two grains (455.8±9.1 and 464.0±8.7 Ma) display characteristic features of magmatic origin, meaning oscillatory growth zoning and $^{232}Th/^{238}U$ ratio values of 0.52 and 0.66, respectively (Fig. 3c). Only one zircon grain gave

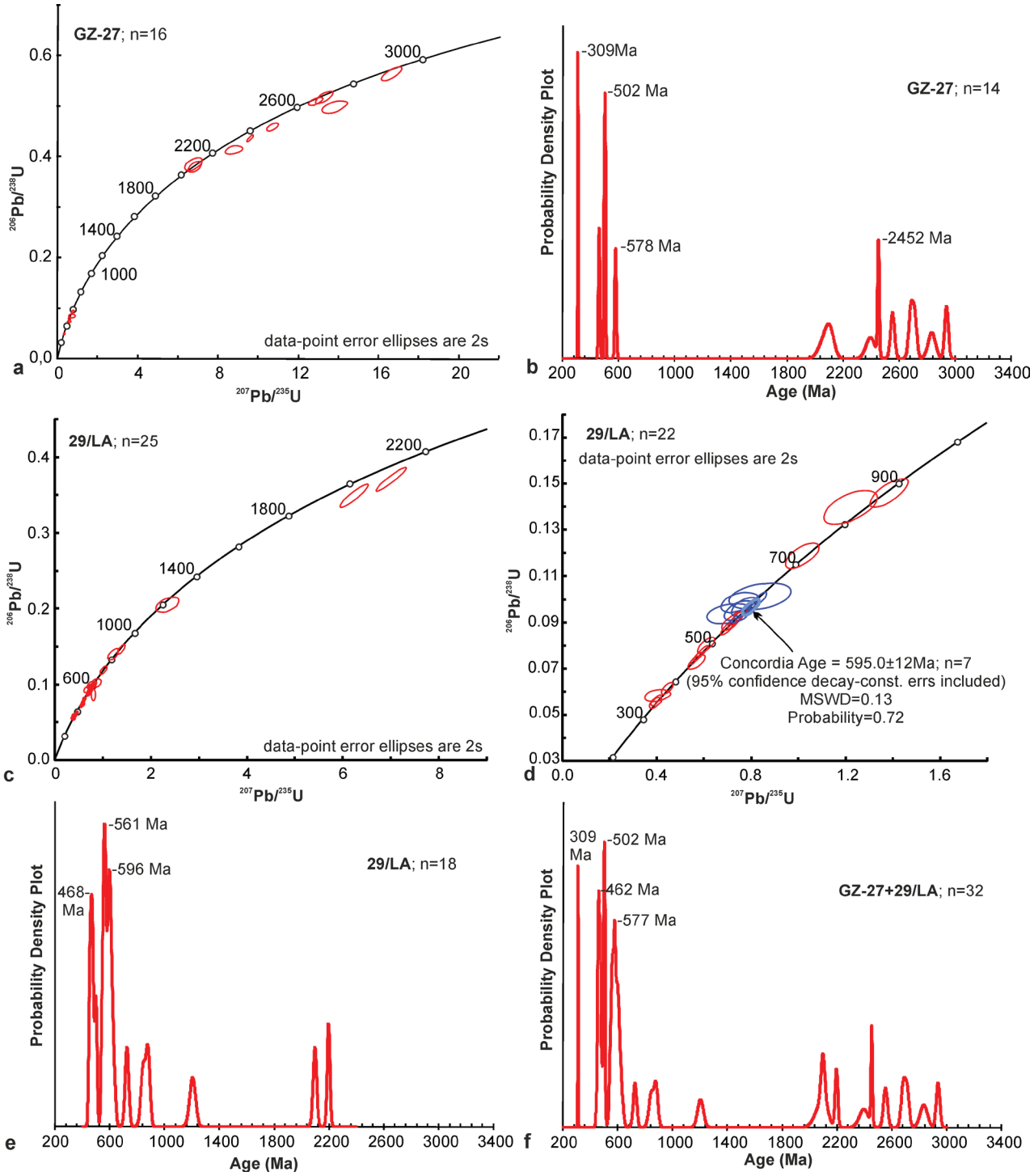

Fig. 7. a — Concordia plots of detrital zircons from the Hámor Fm., sample *GZ-27*. **b** — Corresponding PDP. **c** — Concordia plot for all dated detrital zircon ages from the sample *29-LA*. **d** — Selected sector for age spectrum from 300 to 900 Ma, with indication of the Concordia age. **e** — Corresponding PDP diagram of all dated zircons from the sample *29-LA*. **f** — PDP diagram of detrital zircon ages from the samples *GZ-27* and *29-LA*.

Furongian age of 493.1±9.4 Ma. Four other detrital zircon grains presented the Precambrian ages, while three of them yielded Tonian–Stenian of 901.0±16, 923.0±17 and 1201.0±31 Ma and the other one a Paleoproterozoic age of 2222.0±12 Ma (Supplement, Table S2).

Thus, the main peak at 350 Ma, accompanied by two subpeaks at 301 and 456 Ma are emphasized on the PDP diagram (Fig. 8).

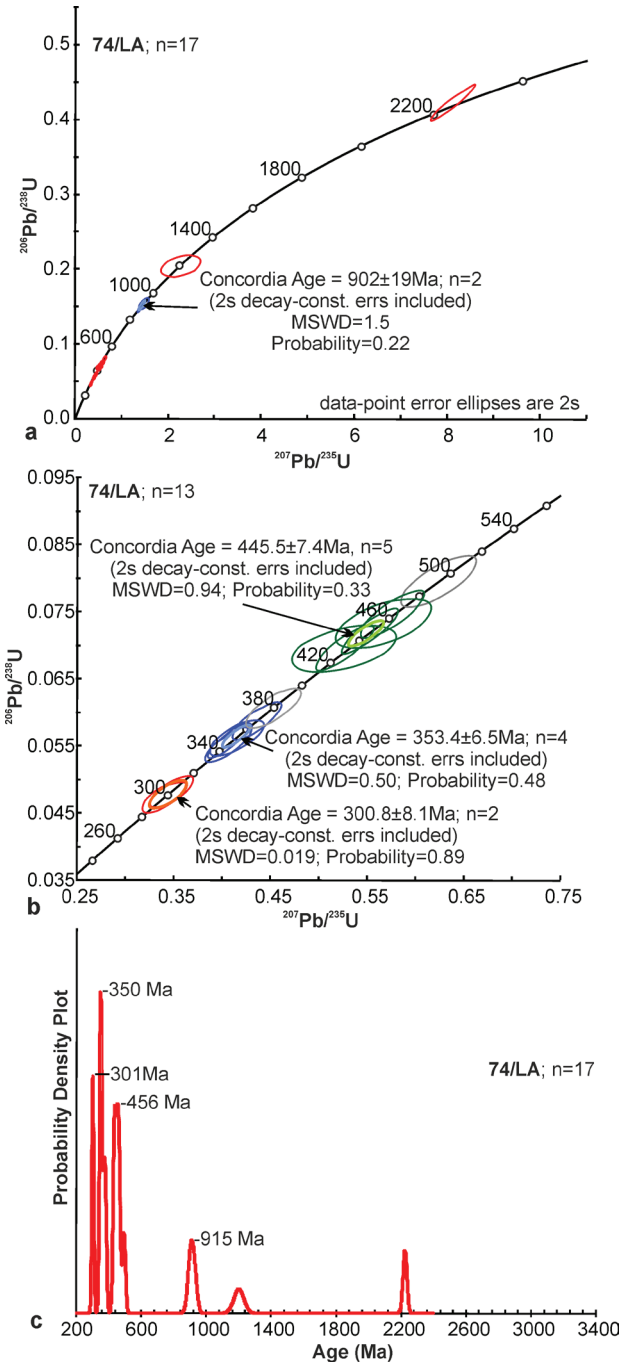

Fig. 8. a — Concordia plot for all detrital zircons from the Petrova Hora Fm., sample *74-LA*. **b** — Selected Concordia for age spectrum from 260 to 540 Ma, with indication of the Concordia ages. **c** — Corresponding PDP.

Novoveská Huta Formation

A detrital zircon analysis from sample ***LA-66*** was first published in the article Vozárová et al. (2013). At present the set of measurements has been completed by the additional data and recalculated. Detrital zircon ages show a relatively good concordance, 30 analysed concordant spots out of 33 (Supplement, Table S2). The Concordia ages, calculated from the cluster along the Concordia curve, show 294.2±6.9 Ma (from seven spots), 363.5±4.5 (from ten spots) and 488.9±8.2 Ma (from five spots) (Fig. 9). The youngest detrital zircon ages are ranging from 275.8±5.9 to 305.9±6.1 Ma. The magmatic origin of this population is confirmed by the $^{232}Th/^{238}U$ ratio values ranging from 0.24 to 0.61 and a characteristic oscillatory growth zoning. Upper Devonian to Mississippian ages ranging from 352.7±6.6 to 379.3±7.4 Ma are dominant. The majority of this detrital zircons group is of magmatic origin, documented by $^{232}Th/^{238}U$ ratios in the range of 0.10–1.12, as well as an oscillatory growth zoning. The only exception is spot 24, determined on the rim of xenocrystic core, with 0.02 value of $^{232}Th/^{238}U$ ratio, indicating the Mississippian/Famennian metamorphic event (356.8±6.7 Ma). Similarly, two spots in the age of 471.3±9.7 and 480.8±9 Ma (Lower Ordovician) were determined within the rims that mantled the strong resorbed xenocrystic cores, with $^{232}Th/^{238}U$ ratio of 0.08 and 0.02, respectively. Another three detrital zircon grains, ranging from 513.0±10 to 495.3±9.3 Ma ages (Upper Cambrian), show the oscillatory zoned internal texture and $^{232}Th/^{238}U$ ratios between 0.21–0.53 that confirm presumably acid magmatic sources. Precambrian detrital zircons are scarcely presented in the studied sample (5 grains). One of these, with the age of 588.0±12 Ma belongs to the Ediacaran, another one of 1502.2±9.8 Ma to the Calymmian, and the last four zircons are Paleoproterozoic–Neoarchean of 2314.0±22, 2653.2±4.2, 2697.3±9.9 and 2725.0±15 Ma.

Whole zircon age spectrum from the sample ***LA-66*** is characterized on the PDP diagram by the dominant peak at 364 Ma, and smaller peaks at 301, 494 and 2655 Ma are revealed (Fig. 9).

Discussion

The age distributions from previous (Vozárová et al. 2013) and recent detrital zircon data are displayed as Kernel Density Estimates (Fig. 10). The whole set of measurements of the Mississippian Hrádok Fm. show the noticeable unimodal distribution with peak at 352 Ma (Fig. 10). The substantial part of the whole studied detrital zircon population was derived from magmatic sources, which is indicated by higher Th/U ratios, ranging from 0.3 to >1. Only three analysed spots in the age of 340±2, 356±7 and 368±4 Ma, from the whole Famennian/Tournaisian zircon assemblage, have typical features of metamorphic origin, with low Th/U ratio values (0.02–0.04) and a weak or absent growth zoning. These spots represent metamorphic cores that are thinly rimmed by magmatic zircons,

indicating a reworking during later stages of the Variscan magmatic cycle. Two metamorphic rims aged of 356 Ma and 565 Ma were found around the older detrital magmatic zircons (2.43 Ga and 2.66 Ga, respectively). This clearly documents the repeated recycling of the old zircon derived from the Paleoproterozoic/Neoarchean crust surpassing a strong Neoproterozoic and Variscan metamorphic overprint.

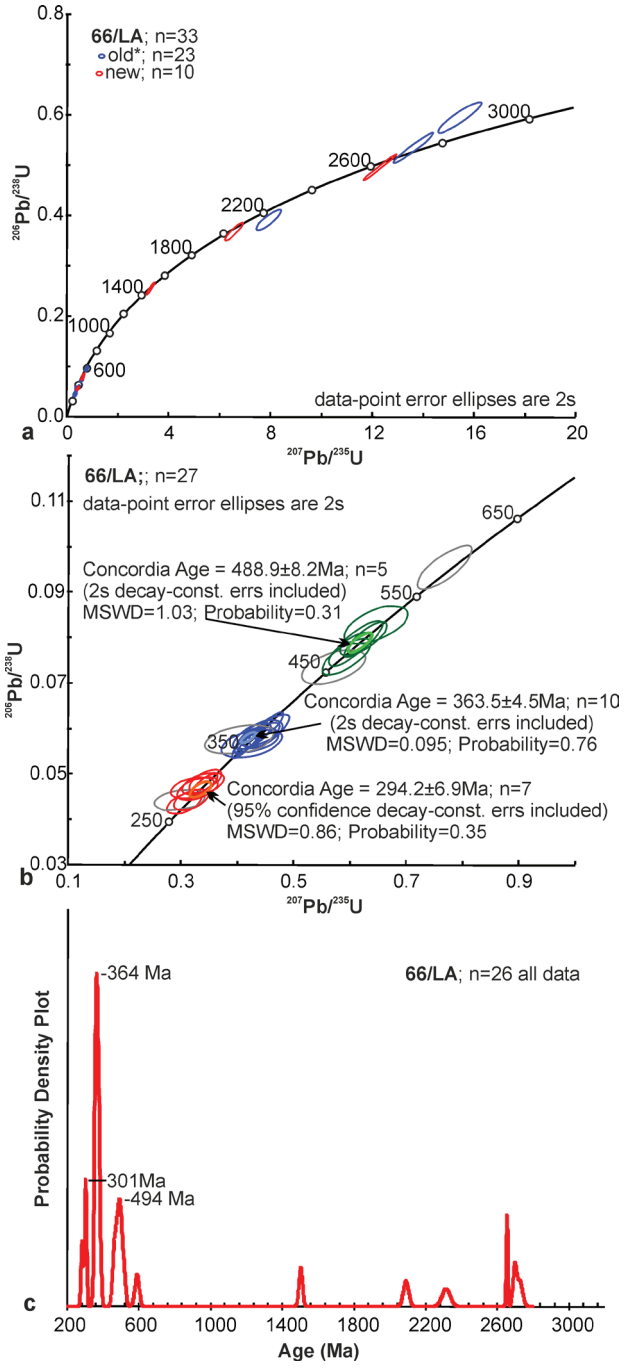

Fig. 9. **a** — Concordia plot of detrital zircons from the Novoveská Huta Fm., sample *LA-66* (old and new data together; old data taken from Vozárová et al. 2013). **b** — Selected Concordia for age spectrum from 250 to 650 Ma, with indication of the Concordia ages. **c** — Corresponding PDP.

Detrital zircon age spectra reflect the tectonic setting of the basin in which the studied sediments were deposited and thus represent major phases of crust formation (Condie et al. 2009; Hawkesworth et al. 2010; Cawood et al. 2012). Large volumes of magma are generated in convergent plate margin settings. Convergent margin basins have a high proportion of detrital igneous zircons (generally greater than 50 %) with unimodal distribution. The crystallization ages are close to the age of host sediments (Cawood et al. 2012). In fact, the 370–344 Ma zircon ages include approximately 75 % from the whole zircon age data of the Hrádok Fm. and the 352 Ma peak age is nearly corresponding to its depositional age (Tournaisian–Visean microfloral assemblages documented by Bajaník & Planderová 1985).

Basins that contain a large number of igneous zircons with ages close to the time of sediment accumulation reflect the setting of the magmatic activity (e.g., forearc, trench, and backarc basins on convergent plate margins) (Dickinson & Gehrels 2009; Condie et al. 2009; Cawood et al. 2012). The presence of zircon grains with ages approximating to the time of accumulation of the host sediments is likely to reflect the proximity of the basin to a plate margin (Hawkesworth et al. 2010). The NGU Mississippian metasedimentary rocks have a unimodal detrital zircon population, which is similar to the depositional age of the Hrádok Fm. The latter sedimentary record shows the detrital zircons clustering within the 352 Ma peak that indicates the main crystallization age of magmatites in the supposed source area. Thus, this unimodal igneous zircon detritus reflects an extensive clastic input from a supposed magmatic arc into the deep-slope Hrádok Fm. basin, situated along an active margin, what is consistent with a convergent margin setting.

Completely different detrital zircon distributions are displayed on the KDE plot from the Pennsylvanian Rudňany and Hámor formations. The basal Rudňany Fm. shows a multimodal distribution, with the peaks at 357, 520, 667, 2021 and 2696 Ma (Fig. 10a). Similarly, detrital zircon populations from the Hámor Fm. display main peaks at 335, 453 and 577 Ma on the KDE plot (Fig. 10a). These patterns reflect the variable amount of zircon detritus derived from the Tournaisian/Famennian syn-collisional magmatism, as well as older ages, reflecting units incorporated in the Variscan orogenic belt. A relatively higher presence of the Cambrian–Ordovician and the Ediacaran–Cryogenian zircon ages and increasing number of the Paleoproterozoic–Neoarchean zircon grains are characteristic. These detrital zircon age spectra correspond to an inconstant and mixed source area that is characteristic for the collisional belt provenance (Dickinson & Gehrels 2009 and references therein). Based on Cawood et al.'s (2012) sedimentary basins classification these originated in connection with continental collision, such as foreland basins (collisional basin type). While between the Pennsylvanian detrital zircon populations the igneous zircon grains are predominant, some of them indicate derivation from the metamorphic sources. These are grouped into several time sections: Upper Devonian–Mississippian in the range of 387–353 Ma, Lower and Upper

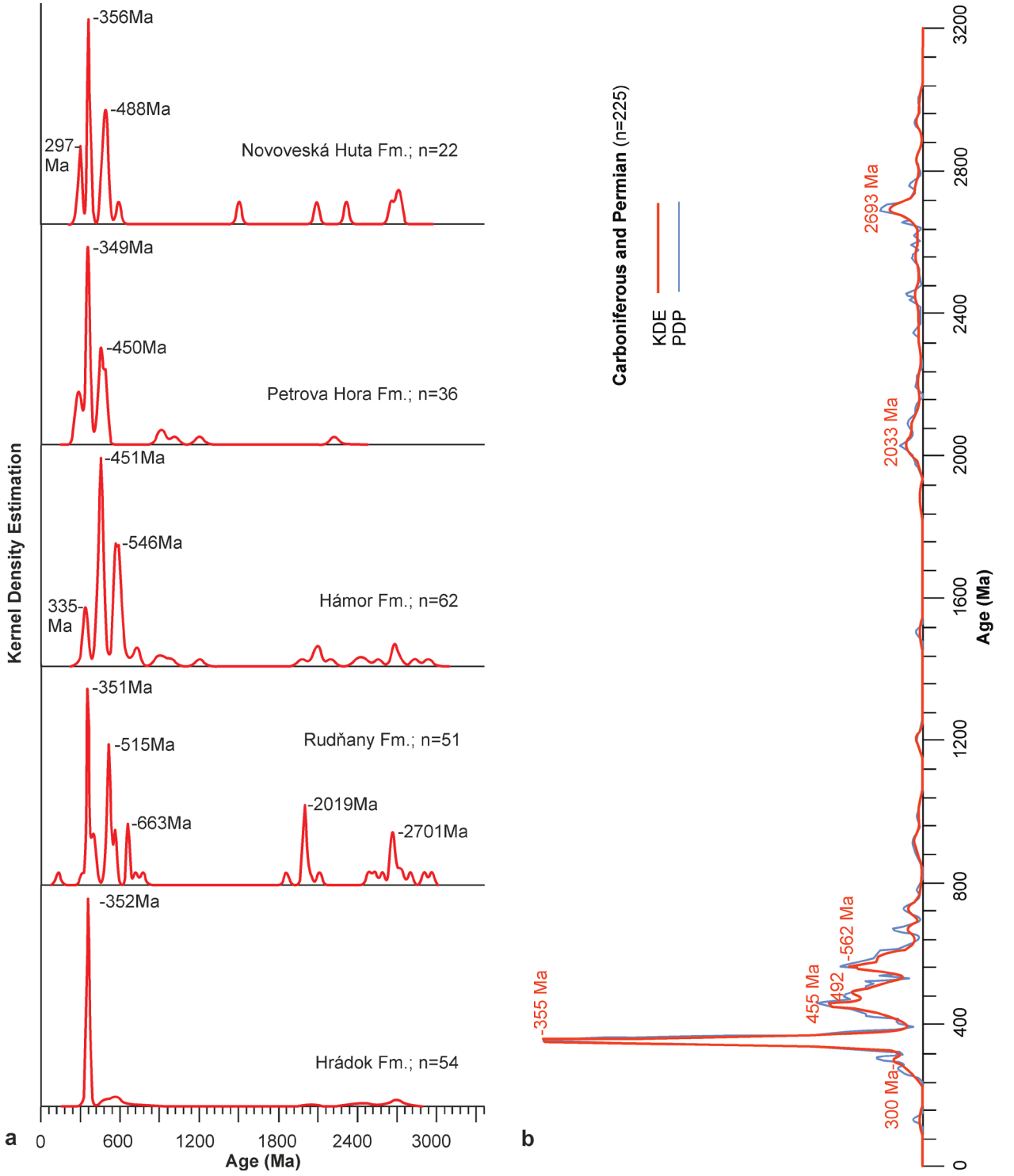

Fig. 10. a — Kernel Density Estimation for the entire detrital zircon populations, with discordant filter of 10 %. **b** — Kernel Density Estimation for the whole studied Carboniferous–Permian detrital zircon population with the corresponding PDP diagram. Note: In the diagrams have been used all measurements, taken from the present data and the paper Vozárová et al. 2013.

Ordovician aged from 476 to 451 Ma and Silurian, aged of 440 and 426 Ma (present paper and Vozárová et al. 2013).

The next group of selected detrital zircons was collected from the Permian red-beds, at the Petrova Hora and Novoveská Huta formations. Both formations reveal nearly similar age peaks on the KDE plot, in the range of Lower/Middle Ordovician (486 vs. 460 Ma) and Mississippian (356 vs. 350 Ma) (Fig. 10). Among detrital zircons the occurrences of the Gzhelian–Asselian igneous zircons in the range from 306±6 to 296±6 Ma are exceptional. A small number of

the Artinskian–Kungurian ages, ranging from 281±6 to 276±6 Ma were identified within the Novoveská Huta Fm. zircon population. They represented reworked zircon grains from the syn-sedimentary volcanic events. In general, the distribution of detrital zircons within both Permian formations reproduce the post-collisional tectonic setting (extensional basins in the sense of Cawood et al. 2012). Small number of zircon ages close to the depositional age of the Permian sedimentary formations (Artinskian–Kungurian) reflect a rift-related magmatic activity.

The presented detrital zircon ages, with the main peaks at 300, 355, 455, 492, 562 and ~2.0 and ~2.7 Ga on the KDE plot (Fig. 10b), specify generally, the provenance of the NGU Carboniferous–Permian sediments from the Western Carpathian Crystalline Basement (WCCB) crust and the pre-Carboniferous complexes of the Northern Gemericum Basement. As the latter complexes consist mainly of the zircon poor rocks (metabasalt, amphibolite, metagabbro, serpentinite, phyllite), the studied detrital zircon population largely reflect derivation from the WCCB crust. This contradicts the petrofacial analysis of the lithic fragments within the NGU Carboniferous–Permian sediments, containing detritus from the NGU pre-Carboniferous complexes predominantly (Vozárová 1973, 1996, 1998a,b; Vozárová & Vozár 1988 and references therein).

The large number of magmatic zircon data, ranging from 370 to 340 Ma, were published from the Tatricum and Veporicum granitoids, which document the evidence of successive I- to S-type granitic magmatism (Bibikova et al. 1988; Kráľ et al. 1997; Poller & Todt 2000; Poller et al. 2000; Putiš et al. 2003; Poller et al. 2005; Kohút et al. 2009; Burda et al. 2011, 2013; Broska et al. 2013; Gawęda et al. 2016). This time interval includes pre-plate and late-orogenic/anatectic events of magmatic activities of the Variscan orogeny. Second important tectono–thermal events, which have been ascertained in the NGU Carboniferous–Permian zircon assemblages are concentrated in the Cambrian–Ordovician time interval that is well documented by detrital zircon ages, ranging from 520 to 453 Ma. This time span fits into the magmatic zircon ages from the Layered Amphibolite Complex (LAC) and different orthogneisses in the WCCB (Putiš et al. 2001, 2003, 2008, 2009a; Gaab et al. 2005, 2006). The Cambrian magmatic zircon ages (Supplement, Table S1; Fig. 5) were also ascertained in the biotite–plagioclase orthogneiss cobble from the Pennsylvanian Rudňany Fm., with expressive metamorphic overprint at 386 Ma in the zircon rims (present paper). This cobble could be derived from the NGU Klátov Complex, in which biotite–plagioclase gneisses are associated with the prevalent amphibolites (Bajaník & Hovorka 1981; Hovorka et al. 1990; Faryad 1986, 1990; Radvanec 1994). The oldest K/Ar radiometric data from the amphibolites gave 324–281 Ma metamorphic age (Kantor et al. 1981). The newest zircon data yielded the magmatic Concordia age at 482±9 Ma with indication of remelting at 383±3 Ma (Putiš et al. 2009a).

In the studied detrital zircon population, metamorphic zircons are scarce and had been noticed either as the rim around the older magmatic cores or as the individual detrital grains. They are concentrated into three-time intervals: i) Upper Devonian/Mississippian in the range of 387–353 Ma; ii) Lower Ordovician in the range of 476–469 Ma; iii) Upper Ordovician–Silurian in the range of 451–426 Ma (present paper and Vozárová et al. 2013). Devonian–Mississippian metamorphic/anatectic ages were described by U–Pb zircon data from the WCCB different orthogneisses, migmatites, metagabbro dolerites, layered amphibolites and leucosome layers in LAC, metatonalites, as well as from metagabbro of the NGU zone (Poller et al. 2000; Poller & Todt 2000; Putiš et al. 2003, 2008, 2009a; Gaab et al. 2005) and CHIME monazite ages from WCCB gneisses and micaschists (Janák et al. 2004). These metamorphic ages are mainly Variscan. A rare 430 Ma metamorphic age was described from the leucotonalite of LAC complex (Putiš et al. 2008).

Generally, the Precambrian zircon ages are presented in the very variable amounts (from 8 % to ~30 %). They are relatively frequent in sedimentary formations deposited after the sedimentation break (Rudňany, Hámor and Novoveská Huta formations). Paleoproterozoic (Orosirian/Rhyacian) and Neoarchean ages of 2.0 Ga and 2.5–2.7 Ga respectively predominate among the Precambrian zircons. This population is well documented in the cobble from the Rudňany Fm. conglomerates (sample ***GZ-36A***) with the main age peaks at 2028 and 2688 Ma and smaller peaks with Lower Cambrian/Late Neoproterozoic ages at 537 and 576 Ma (Fig. 5). As the youngest zircons are Lower Cambrian, the supposed age of this quartzite rock could be Upper Cambrian/Ordovician which corresponds well with the "Armorican Quartzite" lithofacies (Henderson et al. 2016; Fernández-Suárez et al. 2002; Linneman et al. 2004, 2014). In general, the Precambrian detrital zircon population from the NGU Carboniferous–Permian sedimentary rocks are concordant with the Smrečinka Fm. detrital zircon population, from the basal part of the Rakovec Group, which is a part of the NGU Variscan basement (Vozárová et al. 2019). This dispersal of detrital zircon ages suggests a linkage with Armorican terranes, which are characterized by derivation from the Cadomian arc that resides on the periphery of the West African Craton of North Gondwana. Reworking of the Eburnian crust (1.8–2.1 Ga) is characteristic. But, the recycling of the small number of Tonian–Stenian (0.8–1.0 Ga) and Grenvillean ages (1.2–1.5 Ga) were ascertained in detrital zircons from the NGU Permian sequences. This zircon population is not characteristic for the Armorican/West African Craton provenance (e.g., Linnemann et al. 2007; Abati et al. 2012; Gärtner et al. 2013, 2016; Henderson et al. 2016). Nevertheless, a small number of Mesoproterozoic ages were also described from the Armorican Quartzites of the Cantabrian Zone of NW Iberia (Fernández-Suárez et al. 2002; Guttiérrez-Alonso et al. 2007), as well as from the Ordovician sandstones of Corsica (Avigad et al. 2018). Perhaps, the presence of Mesoproterozoic zircons in the NGU Pennsylvanian–Permian sequence, at least in small proportions, indicates a possible presence of the pre-Neoproterozoic crustal vestiges that were accreted within the Western Carpathian Variscan

orogenic domain. Another possibility is the derivation from the Southern Gemericum basement, in which Tonian–Stenian zircon ages are relatively common, but the Grenvillean-aged zircons are absent or their presence is negligible (Vozárová et al. 2012, 2017). Equally, the presence of the Variscan magmatic zircons is the considerable difference between the NGU Carboniferous–Permian and SGU Permian detrital zircon populations. While in the NGU Carboniferous–Permian sediments these igneous zircons occur continuously in all formations, in the SGU Permian they are present only in the upper lithostratigraphic unit (Štítnik Fm.; Vozárová et al. 2012). But that would presume the large transform emplacement of the SGU basement, in which it was incorporated into the Variscan collisional belt in the Permian.

Conclusion

The detrital zircon age patterns of the Carboniferous–Permian sedimentary basins in the Northern Gemericum were controlled by tectonic settings, connected with the gradual closing of the Variscan collisional suture.

The Mississippian detrital zircon population is characterized by its unimodal distribution, with a sharp age peak at 352 Ma. Among those, the dominant portion is represented by detrital zircons of igneous origin, with ages close to the depositional age of the host sediments, which is consistent with a convergent plate margin setting. The Mississippian basin reflects derivation from a magmatic arc that was nearly coeval with accumulation of the sediments.

The Pennsylvanian detrital zircon population is distinctive because of the multimodal distribution and increased amount of Neoproterozoic and Neoarchean ages. This pattern reflects the variable amount of zircon detritus from syn-collisional magmatism (peaks at 335 and 357 Ma) and the pre-existing magmatic rocks associated with opening of the Rakovec sedimentary trough (from 453 to 520 Ma), as well as a band of older ages (577–667 Ma and 2021–2696 Ma, respectively), reflecting the units caught in the Variscan orogenic belt. The Pennsylvanian basin was formed during continental collision, in the foreland setting.

Basically, the same trend in the distribution of detrital zircons was also found in the Permian sediments. The only difference is the presence of younger magmatic ages, from Kasimovian/Gzhelian to Asselian (306–294 Ma) and Artinskian–Kungurian (280–276 Ma). This pattern reflects a post-collisional, extensional type of sedimentary basin. Zircons with ages close to the depositional age of the Permian formations reflect rift-related magmatic activity.

Acknowledgements: The financial support of the Slovak Research and Development Agency (projects ID: APVV-0546-11 and APVV-0146-16) and of the Scientific Grant Agency of the Ministry of Education of the Slovak Republic and the Slovak Academy of Sciences (project VEGA 2/0006/19) is gratefully appreciated. The authors would like to thank U. Klötzli and Z. Németh for constructive reviews and for their helpful and critical comments which led to significant improvement of an earlier versions of the manuscript.

References

Abati J., Aghzer A.M., Gerdes A. & Ennih N. 2012: Insights on the crustal evolution of the West African Craton from Hf isotopes in detrital zircons from Anti-Atlas belt. *Precambrian Res.* 212–213, 263–274.

Abonyi A. 1971: Stratigraphic and tectonic evolution of the Gemeric Carboniferous west from the Štítnik Fault. *Geol. Práce, Spr.* 57, 339–348 (in Slovak).

Andrusov D. 1959: Geology of the Czechoslovak Western Carpathians, 2nd part. *VEDA Publishing House*, Bratislava, 1–376 (in Slovak).

Avigad D., Rossi Ph., Gerdes A. & Abdo A. 2018: Cadomian metasediments and Ordovician sandstones from Corsica: detrital zircon U–Pb–Hf constraints on their provenance and paleogeography. *Int. J. Earth Sci. (Geol. Rundsch.)* 107, 2803–2818. https://doi.org/10.1007/s00531-018-1629-3

Bajaník Š. & Hovorka D. 1981: The amphibolite facies metabasites of the Rakovec Group of Gemericum (West Carpathians). *Geol. Zborn. Geol. Carpath*. 32, 6, 679–705.

Bajaník Š., Vozárová A. & Reichwalder P. 1981: Lithostratigraphic classification of Rakovec Group and Late Paleozoic sediments in the Spišsko-gemerské rudohorie Mts. *Geol. Práce, Spr.* 75, 27–56 (in Slovak).

Bajaník Š., Hanzel V., Ivanička J., Mello J., Pristaš J., Reichwalder P., Snopko L, Vozár J. & Vozárová A. 1983: Explanation to geological map of the Slovenské rudohorie Mts. – eastern part. *D. Štúr Inst. Geol. Publ. House*, Bratislava, 3–223 (in Slovak with English summary).

Bajaník Š., Ivanička J., Mello J., Pristaš J., Reichwalder P., Snopko L., Vozár J. & Vozárová A. 1984a: Geological map of the Slovenské rudohorie Mts. – eastern part, 1:50 000. *D. Štúr Inst. Geol.*, Bratislava.

Bajaník Š., Vozárová A., Snopková P. & Straka P. 1984b: Lithostratigraphy of the Črmeľ Group. *Manuscript No. 58729, Archives D. Š. Inst. Geology*, Bratislava, 1–90 (in Slovak).

Bajaník Š. & Planderová E. 1985: Stratigraphic position of the lower part of the Ochtiná Formation (between Magnezitovce and Magura). *Geol. Práce, Spr.* 82, 67–76 (in Slovak).

Bibikova E.V., Cambel B., Korikovsky S.P., Broska I., Gracheva T.V., Makarov V.A. & Arakeliants M.M. 1988: U–Pb and K–Ar isotopic dating of Sinec (Rimavica granites) (Kohút zone of Veporides). *Geol. Zborn. Geol. Carpath*. 39,147–157.

Biely A., Bezák V., Elečko M., Gross P., Kaličiak M., Konečný V., Lexa J., Mello J., Nemčok J., Potfaj M., Rakús M., Vass D., Vozár J. & Vozárová A. 1996a: Explanation to geological map of Slovakia, 1:500 000. *Dionýz Štúr Publisher*, Bratislava, 1–76.

Biely A., Bezák V., Elečko M., Gross P., Kaličiak M., Konečný V., Lexa J., Mello J., Nemčok J., Potfaj M., Rakús M., Vass D., Vozár J. & Vozárová A. 1996b: Geological map of Slovakia: *Ministry Environm. Slovak Republic, Geol. Surv. Slovak Republic,* Bratislava.

Black L.P., Kamo S.L., Allen C.M., Aleinikoff J.N., Davis D.W., Korsch R.J. & Foudoulis C. 2003: TEMORA 1: a new zircon standard for Phanerozoic U–Pb geochronology. *Chem. Geol.* 200, 155–170. https://doi.org/10.1016/S0009-2451(03)00165-7

Bouček B. & Přibyl A. 1960: Revision der Trilobiten aus dem slowakischen Oberkarbon. *Geol. Práce, Spr*. 20, 5–50 (in Czech, German summary).

Broska I., Petrík I., Be′eri-Shlevin Y., Majka J. & Bezák V. 2013: Devonian/Mississippian I-type granitoids in the Western Carpathians: A subduction-related hybrid magmatism. *Lithos* 162–163, 27–36.

Burda J., Gawęda A. & Klötzli U. 2011: Magma hybridization in the Western Tatra Mts. granitoid intrusion (S-Poland, Western Carpathians). *Mineral. Petrol.* 103, 1–4, 19–36.

Burda J, Gawęda A. & Klötzli U 2013: Geochronology and petrogenesis of granitoid rocks from the Goryczkowa Unit, Tatra Mountains (Central Western Carpathians). *Geol. Carpath.* 64, 6, 419–435. https://doi.org/10.2478/geoca-2013-0029

Cawood P.A., Hawkesworth C.J. & Dhuime P. 2012: Detrital zircon record and tectonic setting. *Geology* 40, 875–878. https://doi.org/10.1130/G32945.1

Condie K.C., Belousova E., Griffin W.L. & Sircombe K.N. 2009: Granitoid events in space and time: Constraints from igneous and detrital zircon age spectra. *Gondwana Res.* 15, 228–242. https://doi.org/10.1016/j.gr.2008.06.001

Dallmeyer R.D., Neubauer F., Handler R., Fritz H., Müller W., Pana D. & Putiš M. 1996: Tectonothermal evolution of the internal Alps and Carpathians: Evidence from $^{40}Ar/^{39}Ar$ mineral and whole rock data. *Eclogae Geol. Helv.* 89, 203–227.

Dallmeyer R.D., Németh Z. & Putiš M. 2005: Regional tectonothermal events in Gemericum and adjacent units (Western Carpathians, Slovakia): Contribution by $^{40}Ar/^{39}Ar$ dating. *Slovak Geol. Mag*. 11, 2–3, 155–163.

Dickinson W.R. & Gehrels G.E. 2009: Use of U–Pb ages of detrital zircons to infer maximum depositional ages of strata: A test against a Colorado Plateau Mesozoic database: *Earth Planet. Sci. Lett.* 288, 115–125. https://doi.org/10.1016/j.epsl.2009.09.013.

Ebner F., Vozárová A., Kovács S., Kräutner H.-G., Krstić B., Szederkényi T., Jamićić D., Balen D., Belak M. & Trajanova M. 2008: Devonian-Carboniferous pre-flysch and flysch environments in the Circum Pannonian Region. *Geol. Carpath.* 59, 159–195.

Faryad S.W. 1986: Metamorphic evolution of paragneisses from Klátov region (Gemericum). *Geol. Zborn. Geol. Carpath.* 39, 6, 729–749.

Faryad S.W. 1990: Gneiss–amphibolite complex of the Gemericum. *Miner. Slov.* 22, 303–318.

Fernández-Suárez J., Gutiérrez-Alonso G. & Jeffries T.E. 2002: The importance of along-margin terrane transport in northern Gondwana: insights from detrital zircon parentage in Neoproterozoic rocks from Iberia and Brittany. *Earth Planet. Sci. Lett.* 204, 75–88.

Gaab A.S., Poller U., Janák M., Kohút M. & Todt W. 2005: Zircon U–Pb geochronology and isotopic characterization for the pre-Mesozoic basement of the Northern Veporic Unit (Central Western Carpathians, Slovakia). *Schweiz. Mineral. Petrogr. Mitt*. 85, 69–88.

Gaab A.S., Janák M., Poller U. & Todt W. 2006: Alpine reworking of Ordovician protoliths in the Western Carpathians: geochronological and geochemical data on the Muráň Gneiss complex. *Lithos* 87, 261–275.

Gärtner A., Villeneuve M., Linnemann U., El Archi A. & Bellon H. 2013: An exotic terrane of Laurussian affinity in the Mauretanides and Souttoufides (Moroccan Sahara). *Gondwana Res.* 24, 687–699.

Gärtner A., Villeneuve M., Linnemann U., Gerdes A., Youbi N., Guillou O. & Rjimati E.-C. 2016: History of the West African Neoproterozoic Ocean: key to the geotectonic history of circum-Atlantic Peri-Gondwana (Adrar Souttouf Massif, Moroccan Sahara). *Gondwana Res*. 29, 1, 220–233.

Gawęda A., Burda J., Klötzli U., Golonka J. & Szopa K. 2016: Episodic construction of the Tatra granitoid intrusion (Central Western Carpatians, Poland/Slovakia): consequences for the geodynamics of Variscan collision and Rheic Ocean closure. *Int. J. Earth Sci. (Geol. Rundsch.)* 105, 1153–1174. https://doi.org/10.1007/s00531-015-1239-2

Grecula M. 1998: Carboniferous of the Črmelicum terrane, Western Carpathians: relics of a fore-arc basin within Alpide Variscides. *Miner. Slov.* 30, 109–136.

Gutiérrez-Alonso G., Fernández-Suárez J., Guttiérrez-Marco J.C., Corfu J. & Suárez M. 2007: U–Pb depositional age for the upper Barrios Formation (Armorican Quartzite facies) in the Cantabrian zone of Iberia: Implication for stratigraphic correlation and paleogeography. In: Linnemann U., Nance R.D., Kraft P. & Zulauf G. (Eds.): The evolution of Rheic Ocean: From Avalonian–Cadomian Active margin to Alleghenian–Variscan Collision. *Geol. Soc. Am., Spec. Pap.* 423, 287–296.

Hawkesworth C. J., Dhuime B., Pietranik A., Cawood P., Kemp T. & Storey C. 2010: The Generation and Evolution of the Continental Crust. *J. Geol. Soc., London* 167, 229–248. https://doi.org/10.1144/0016-76492009-072

Henderson B.J., Collins W.J., Murphy J.B., Gutiérrez-Alonso G. & Hand M. 2016: Gondwanan basement terranes of the Variscan Appalachian orogen: Baltican, Saharan and West African hafnium isotopic fingerprints in Avalonia, Iberia and the Armorican Terranes. *Tectonophysics* 681, 278–304.

Hiess J., Condon DJ., McLean N. & Noble SR. 2012: $^{238}U/^{235}U$ systematics in terrestrial uranium-bearing minerals. *Science* 335, 1610–1614.

Hovorka D., Ivan P., Jilemnická I. & Spišiak J. 1988: Petrology and geochemistry of metabasalts from Rakovec (Paleozoic of Gemeric Unit, Inner Western Carpathians). *Geol. Zborn. Geol. Carpath.* 39, 395–425.

Hovorka D., Ivan P. & Spišiak J. 1990: Lithology, Petrology, Metamorphism and Tectonic position of the Klátov Group (Paleozoic of the Gemer unit, Inner Western Carpathians). *Acta Geol. Geogr. Univ. Comenianae, Geol*. 45, 45–68.

International Commission on Stratigraphy. International Chronostratigraphic Chart v 2018/08. http://www.stratigraphy.org/ICSchart/ChronostratChart 2018-08.pdf

Ivan P. 1997: Rakovec and Zlatník Formations: two different relics of the pre-Alpine back-arc basin crust in the Central Western Carpathians. In: Grecula P., Hovorka D. & Putiš M. (Eds.): Geological Evolution of the Western Carpathians. *Miner. Slov., Monograph*, Bratislava, 281–288.

Ivan P. 2009: Early Palaeozoic basic volcanism of the Western Carpathians: geochemistry and geodynamic position. *Acta Geol. Univ. Comenianae*, *Monographic serie, Comenius University*, Bratislava, 7–110 (in Slovak).

Ivan P. & Méres Š. 2012: The Zlatník Group – Variscan ophiolites on the northern border of the Gemeric Superunit (Western Carpathians). *Miner. Slov.* 44, 39–56.

Janák M., Konečný P., Siman P. & Holický I. 2004: A metamorphic history from electron microprobe dating of monazite: Variscan evolution of The Tatra Mountains. *Geolines* 17, 47–48.

Kantor J., Bajaník Š. & Hurný J. 1981: Radiometric dating of metamorphites of amphibolite facies from the Rudňany Deposits, Spišsko-gemerské rudohorie Mts. *Geol. Zborn. Geol. Carpath.* 32, 335–344.

Kohút M., Uher P., Putiš M., Ondrejka M., Sergeev S., Larionov A. & Paderin I. 2009: SHRIMP U–Th–Pb zircon dating of the granitoid massifs in the Malé Karpaty Mountains (Western Carpathians): evidence of Meso-Hercynian successive S- to I-type granitic magmatism. *Geol. Carpath.* 60, 5, 345–350.

Kohút M., Trubač J., Novotný L., Ackerman L., Demko R., Bartalský B. & Erban V. 2013: Geology and Re-Os molybdenite geochronology of the Kuríšková U–Mo deposit (Western Carpathians, Slovakia). *J. Geosci.* 58, 275–286. https://doi.org/10.3190/jgeosci.150

Kozur H., Mock R. & Mostler H. 1976: Stratigraphische Neueinstufung der Karbonatgesteine der unteren Schichtenfolgen von Ochtiná (Slovakei) in das oberste Vise-Serpukhovian (Namur A). *Geol. Palaeont. Mitt*. 6, l, 1–29.

Kozur H. & Mock R. 1977: Erster Nachweis von Conodonten im Paleozoikum (Karbon) der Westkarpaten. *Čas. pro miner. geol*. 22, 3, 299–305.

Kráľ J., Hess J.C., Kober B. & Lippolt H.J. 1997: $^{207}Pb/^{206}Pb$ and $^{40}Ar/^{39}Ar$ data from plutonic rocks of the Strážovské vrchy Mts. basement, Western Carpathians. In: Grecula P., Hovorka D. & Putiš M. (Eds.): Geological evolution of the Western Carpathians. *Mineralia Slovaca – Monograph*, Bratislava, 253–260.

Krist E. 1954: Bindt–Rudňany conglomerates, Carboniferous of the northern part of the Slovenské Rudohorie Mts. *Geol. Práce, Zošit* 36, *Dionýz Štúr Inst. Geology*, Bratislava, 77–107 (in Slovak).

Lexa O., Schulmann K. & Ježek J. 2003: Cretaceous collision and indentation in the West Carpathians: View based on structural analysis and numerical modelling. *Tectonics* 22, 6, 1066. https://doi.org/10.1029/2002TC001472

Linnemann U., McNaughton N.J., Romer R.L., Gehmlich M., Drost K. & Tonk C. 2004: West African provenance for Saxo-Thuringia (Bohemian Massif): did Armorica ever leave pre-Pangean Gondwana? U/Pb SHRIMP zircon evidence and Nd-isotopic record. *Int. J. Earth Sci. (Geol. Rundsch.)* 93, 683–705.

Linnemann U., Gerdes A., Drost K. & Buschmann B. 2007: The continuum between Cadomian orogenesis and opening of the Rheic Ocean: constraints of the LA-ICP-MS zircon dating and analyses of plate-tectonic setting, Saxo–Thuringian zone, northeastern Bohemian Massif, Germany. *Geol. Soc. Am. Spec. Pap.* 423, 61–96.

Linnemann U., Gerdes A., Hofmann M. & Marko L. 2014: The Cadomian Orogen: Neoproterozoic to Early Cambrian crustal growth and orogenic zoning along the periphery of the West African Craton – Constraints from U–Pb zircon ages and Hf isotopes (Schwarzburg Antiform, Germany). *Precambrian Res.* 244, 236–278.

Ludwig K.R. 2005: SQUID 1.12 A User's Manual. A Geochronological Toolkit for Microsoft Excel. *Berkeley Geochronology Centre Special Publication,* 1–22. http://www.bgc.org/klprogrammenu.html

Ludwig K.R. 2012: User's Manual for Isoplot 3.75. A geochronological Toolkit for Microsoft Excel. *Berkeley Geochronology Centre Special Publication* 5, 1–71. http://www.bgc.org/isoplot.html

Mamet B. & Mišík M. 2003: Marine Carboniferous algae from metacarbonates of Ochtiná Formation (Gemeric Unit, Western Carpathians). *Geol. Carpath.* 54, 3–8.

Michalík J. (Ed.) 2007: Stratigraphic manual. Slovak stratigraphic terminology, stratigraphic classification and method. *VEDA*, *Slovak Academy of Sciences*, Bratislava, 1–166 (in Slovak).

Němejc F. 1947 Contribution to knowledge of floral remnants and stratigraphical division of Permo-Carboniferous of Slovakia. *Rozpravy II. Čes. Akad. Věd* 56, 15, Praha, 1–34 (in Czech).

Németh Z. 2002: Variscan suture zone in Gemericum: Contribution to reconstruction of geodynamic evolution and metallogenic events of Inner Western Carpathians. *Slovak Geol. Mag.* 8, 247–257.

Németh Z., Procházka W., Radvanec M., Kováčik M., Madarás J., Koděra P. & Hraško Ľ. 2004: Magnesite and talc origin in the sequence of geodynamic events in Veporicum, Inner Western Carpathians. *Acta Petrol. Sinica* 20, 837–854.

Novotný L. & Miháľ F. 1987: New lithostratigraphic units of the Krompachy Group. *Miner. Slov.* 19, 97–113 (in Slovak).

Novotná N., Jeřábek P., Pitra P., Lexa O. & Racek M. 2015: Repeated slip along a major decoupling horizon between crustal scale nappes of the Central Western Carpathians documented in the Ochtiná tectonic mélange. *Tectonophysics* 646, 50–64.

Neubauer F. & Vozárová A. 1990: The Noetsch-Veitsch-Northgemeric Zone of Alps and Carpathians: Correlation, paleogeography and significance for Variscan orogeny. In: Minaříková D. & Lobitzer H. (Eds.): Thirty years of geological cooperation between Austria and Czechoslovakia. *Federal Geol. Surv.*, Vienna, 167–171.

Planderová E. & Vozárová A. 1982: Biostratigraphical correlation of the Late Paleozoic formations in the West Carpathians. In: Sassi F.P. (Ed.): Newsletter No. 4, IGCP Project No. 5, Padova, 67–71.

Plašienka D., Grecula P., Putiš M., Kováč M. & Hovorka D. 1997: Evolution and structure of the Western Carpathians: an overview. In: Grecula P., Hovorka D., Putiš M. (Eds.): Geological evolution of the Western Carpathians. *Miner. Slov, Monograph*, Bratislava, 1–24

Plašienka D. 2018: Continuity and episodicity in the early Alpine tectonic evolution of the Western Carpathians: How large-scale processes are expressed by the orogenic architecture and rock record data. *Tectonics* 37, 2029–2079. https://doi.org/10.1029/2017TC004779

Poller U. & Todt W. 2000: U–Pb single zircon data of granitoids from the High Tatra Mountains (Slovakia): implications for the geodynamic evolution. *Geol. Soc. Am. Spec. Pap.* 350, 235–243.

Poller U., Janák M., Kohút M. & Todt W. 2000: Early Variscan magmatism in the Western Carpathians: U–Pb zircon data from granitoids and orthogneisses of the Tatra Mountains (Slovakia). *Int. J. Earth Sci. (Geol. Rundsch.)* 89, 2, 336–349. https://doi.org/10.1007/s005310000082

Poller U., Kohút M., Anders B. & Todt W. 2005: Multistage geochronological evolution of the Veľká Fatra Mts. – a combined TIMS and ion-microprobe study on zircons. *Lithos* 82, 113–124.

Putiš M., Kotov A.B., Korikovsky S.P., Salnikova E.B., Yakovleva S.Z., Berezhnaya N.G., Kovach V.P. & Plotkina J.V. 2001: U–Pb zircon ages of dioritic and trondhjemitic rocks from a layered amphibolitic complex crosscut by granite veins (Veporic basement, Western Carpathians). *Geol. Carpath.* 52, 1, 49–60.

Putiš M., Kotov A. B., Petrík I., Korikovsky S. P., Madarás J., Salnikova E.B., Yakovleva S.Z., Berezhnaya N.G., Plotkina Y.V., Kovach V.P., Lupták B. & Majdán M. 2003: Early– vs. Late orogenic granitoids relationships in the Variscan basement of the Western Carpathians. *Geol. Carpath.* 54, 163–174.

Putiš M., Sergeev S., Ondrejka M., Larionov A., Siman P., Spišiak J., Uher P. & Paderin I. 2008: Cambrian–Ordovician metaigneous rocks associated with Cadomian fragments in the West-Carpathian basement dated by SHRIMP on zircons: a record from the Gondwana active margin setting. *Geol. Carpath.* 59, 1, 3–18.

Putiš M., Ivan P., Kohút M., Spišiak J., Siman P., Radvanec M., Uher P., Sergeev S., Larionov A., Méreš Š., Demko R. & Ondrejka M. 2009a: Meta-igneous rocks of the West-Carpathian basement, Slovakia: indicators of Early Paleozoic extension and shortening events. *Bull. Soc. Géol. Fr.* 180, 6, 461–471.

Putiš M., Frank W., Plašienka D., Siman P., Sulák M. & Biroň A. 2009b: Progradation of the Alpidic Central Western Carpathians orogenic wedge related to two subductions: constrained by $^{40}Ar/^{39}Ar$ ages of white micas. *Geodyn. Acta* 22, 1–3, 31–56.

Radvanec M. 1994: Petrology of the Gemeric gneiss-amphibolite complex, northern part of the Rudňany deposits. Part I: P–T–x conditions and zonality of metamorphism. *Miner. Slov.* 26, 223–238.

Radvanec M., Németh Z., Kráľ J. & Pramuka S. 2017: Variscan dismembered metaophiolite suite fragments of Paleo-Tethys in Gemeric unit, Western Carpathians. *Miner. Slov.* 49, 1–48.

Rakusz Gy. 1932: Die oberkarbonischen Fosilien von Dobšiná und Nagyvisnyó. *Geol. Hungarica, serie Paleont.* 8, 1–219.

Rakús M., Potfaj M. & Vozárová A. 1998: Basic paleogeographic and paleotectonic units of the Western Carpathians. In: Rakús M. (Ed.): Geodynamic development of the Western Carpathians. *D. Štúr Publ.*, Bratislava, 15–26.

Rojkovič I. & Konečný P. 2005: Th–U–Pb dating of monazite from the Cretaceous uranium vein mineralization in the Permian rocks of the Western Carpathians. *Geol. Carpath.* 56, 493–502.

Rojkovič I. & Mihál' F. 1991: Geological structure and uranium mineralization in Permian of the north-eastern part of the Slovenské Rudohorie Mts. *Miner. Slov.* 23, 123–132 (in Slovak with English summary).

Rojkovič I. & Vozár J. 1972: Contribution to the relationship of the Permian volcanism in the northern Gemerides and Choč Unit. *Geol. Zborn. Geol. Carpath*. 23, Bratislava, 87–98.

Spišiak J., Hovorka D. & Ivan P. 1985: Klátov Group the representative of the Paleozoic amphibolite facies metamorphites of the Inner Western Carpathians. *Geol. Práce, Spr.* 82, 205–220 (in Slovak with English summary).

Steiger R.H. & Jäger E. 1977: Subcommission on geochronology: Convention on the use of decay constants in geo- and cosmochronology. *Earth Planet. Sci. Lett.* 36, 359–362.

Václav J. & Vozárová A. 1978: Characteristic of the Northern Gemeride Permian at Košická Belá. *Záp. Karpaty, Sér. Min. Petr. Geochem. Metalog*. 5, 83–108 (in Slovak).

Vermeesch P. 2012: On the visualization detrital age distributions. *Chem. Geol.* 312–313, 190–194. https://doi.org/10.1016/j.chemgeo.2012.04.021

Vozárová A. 1973: Pebble analysis of the late Paleozoic conglomerates in Spišsko-Gemerské rudohorie Mts. *Geol. Zborn. Západné Karpaty* 18, 7–98 (in Slovak).

Vozárová A. 1996: Tectono-sedimentary evolution of Late Paleozoic basins based on interpretation of lithostratigraphic data (Western Carpathians; Slovakia). *Slovak Geol. Mag.* 3–4, 251–271.

Vozárová A. 1997: Upper Permian-Lower Triassic evaporites in the Western Carpathians (Slovakia). *Slovak Geol. Mag.* 3, 223–230.

Vozárová A. 1998a: Late Hercynian development in the Central Western Carpathians. In: Rakús M. (Ed.): Geodynamic development of the Western Carpathians. *Geol. Surv. Slovak Rep., Dionýz Štúr Publishers,* 41–46.

Vozárová A. 1998b: Late Hercynian development in the Inner Western Carpathians. In: Rakús M. (Ed.): Geodynamic development of the Western Carpathians. *Geol. Surv. Slovak Rep., Dionýz Štúr Publishers,* 75–80.

Vozárová A. 2001: Plagiogranite pebbles in Westphalian conglomerates of the Northern Gemericum Unit: their characteristic and geotectonic significance (Western Carpathians). *Krystalinikum* 27, 79–88.

Vozárová A. & Vozár J. 1988: Late Paleozoic in West Carpathians. *Monogr., D. Štúr. Inst. Geol.*, Bratislava, 1–314.

Vozárová A., Frank W., Kráľ J. & Vozár J. 2005: $^{40}Ar/^{39}Ar$ dating of detrital mica from the Upper Paleozoic sandstones in the Western Carpathians (Slovakia). *Geol. Carpath.* 56, 6, 463–472.

Vozárová A., Šarinová K., Rodionov N., Laurinc D., Paderin I., Sergeev S. & Lepekhina E. 2012: U–Pb ages of detrital zircons from Paleozoic metasandstones of the Gelnica Terrane (Southern Gemeric Unit, Western Carpathians, Slovakia): evidence for Avalonian–Amazonian provenance. *Int. J. Earth Sci. (Geol. Rundsch.*) 101, 919–936. https://doi.org/10.1007/s00531-011-0705-8

Vozárová A., Laurinc D., Šarinová K., Larionov A., Presnyakov S., Rodionov N. & Paderin I. 2013: Pb ages of detrital zircons in relation to geodynamic evolution: Paleozoic of the Northern Gemericum (Western Carpathians, Slovakia). *J. Sediment. Res.* 83, 915–927. https://doi.org/10.2110/jsr.2013.66

Vozárová A., Presnyakov S., Šarinová K. & Šmelko M. 2015: First evidence for Permian-Triassic boundary volcanism in the Northern Gemericum: geochemistry and U-Pb zircon geochronology. *Geol. Carpath.* 66, 5, 375–391.

Vozárová A., Rodionov N., Šarinová K. & Presnyakov S. 2017: New zircon ages on the Cambrian–Ordovician volcanism of the Southern Gemericum basement (Western Carpathians, Slovakia): SHRIMP dating, geochemistry and provenance. *Int. J. Earth Sci. (Geol. Rundsch.)* 106, 2147–2170. https://doi.org/10.1007/s00531-016-1420-2

Vozárová A., Rodionov N. & Šarinová K. 2019: Recycling of Paleoproterozoic and Neoproterozoic crust recorded in Lower Paleozoic metasandstones (Western Carpathians, Slovakia): evidence from detrital zircons. *Geol. Carpath.* 70, 298–310.

Wiedenbeck M., Allé P., Corfu F., Griffin W.L., Meier M., Oberli F., von Quadt A., Roddick J.C. & Spiegel W. 1995: Three natural zircon standards for U–Th–Pb, Lu–Hf, trace element and REE analyses. *Geostand. Newslett.* 19, 1–23.

Williams I.S. 1998: U–Th–Pb geochronology by ion microprobe. In: McKissen M.A., Shanks III W.C. & Ridley W.S. (Eds.): Applications of microanalytical techniques to understanding mineralizing processes. *Rev. Econ. Geol.* 7, 1–35.

Zágoršek K. & Macko A. 1994: Carboniferous Bryozoa from the Jedlovec quarry in Ochtiná Formation (Gemericum, Western Carpathians): *Miner. Slov.* 26, 5, 335–346.

Supplement

Table S1: Microprobe analyses of plagioclases and garnets from the sample GZ-55.

Plagioclase

No	**16 / 1**	**17 / 1**	**19 / 1**	**21 / 1**	**23 / 1**
Sample	**GZ-55**	**GZ-55**	**GZ-55**	**GZ-55**	**GZ-55**
Mineral	**pl**	**pl**	**pl**	**pl**	**pl**
Ana No.	**an1**	**an2**	**an4**	**an6**	**an8**
SiO2	62.94	62.86	63.63	62.16	62.57
Al2O3	23.54	22.63	22.24	23.10	23.36
FeO	0.05	0.00	0.01	0.02	0.00
CaO	5.33	4.72	4.34	5.32	5.17
Na2O	8.41	8.84	8.96	8.21	8.44
K2O	0.18	0.08	0.22	0.20	0.06
SrO	0.05	0.04	0.00	0.05	0.03
Total	100.50	99.17	99.41	99.06	99.63
apfu (8 oxygen)					
Si	2.774	2.803	2.827	2.778	2.778
Al	1.223	1.189	1.165	1.217	1.222
Fe	0.002	0.000	0.000	0.001	0.000
Ca	0.252	0.225	0.206	0.255	0.246
Sr	0.001	0.001	0.000	0.001	0.001
Na	0.719	0.764	0.772	0.711	0.727
K	0.010	0.005	0.012	0.012	0.003
SUM	4.980	4.987	4.983	4.975	4.977
endmembers (%)					
Or	1.05	0.48	1.26	1.18	0.34
Ab	73.29	76.84	77.91	72.75	74.47
An	25.66	22.69	20.84	26.06	25.19

Garnet

No.	**18 / 1**	**20 / 1**	**22 / 1**
Sample	**GZ-55**	**GZ-55**	**GZ-55**
Mineral	**grt**	**grt**	**grt**
Ana No.	**an3**	**an5**	**an7**
SiO2	38.06	37.80	37.79
TiO2	0.01	0.00	0.00
Al2O3	21.11	21.11	21.04
Cr2O3	0.03	0.01	0.01
MgO	2.20	2.15	2.16
FeO	31.63	32.22	32.48
MnO	1.98	2.15	2.43
CaO	6.38	5.61	5.22
Na2O	0.04	0.00	0.03
Total	101.43	101.06	101.16
apfu (8 cations)			
Si	3.007	3.004	3.003
Tetr. Al	0.000	0.000	0.000
sum T	3.007	3.004	3.003
Fe3+	0.033	0.021	0.029
Oct. Al	1.965	1.978	1.971
Cr	0.002	0.001	0.001
Ti	0.000	0.000	0.000
sum X	2.000	2.000	2.000
Fe2+	2.056	2.119	2.129
Ca	0.540	0.478	0.444
Mg	0.259	0.255	0.256
Mn	0.132	0.145	0.164
Na	0.006	0.000	0.004
sum Y	2.993	2.996	2.997
endmembers (%)			
Prp	8.67	8.50	8.55
Sps	4.43	4.83	5.48
Alm	68.81	70.72	71.13
Adr	1.64	1.07	1.45
Grs	16.44	14.87	13.40

Table S2: New U–Pb (SHRIMP) detrital zircon age data from the Carboniferous–Permian sedimentary formations of the Northern Gemericum. Note: the old zircon age data from the sample LA-66, taken from Vozárová et al. 2013, are shaded.

Hrádok Fm.

Spot	% $^{206}Pb_c$	ppm U	ppm Th	$^{232}Th/^{238}U$	ppm $^{206}Pb^*$	(1) $^{206}Pb/^{238}U$ Age	±1s err	(1) $^{207}Pb/^{206}Pb$ Age	±1s err	% Discordant	(1) $^{238}U/^{206}Pb^*$	±%	(1) $^{207}Pb^*/^{206}Pb^*$	±%	(1) $^{207}Pb^*/^{235}U$	±%	(1) $^{206}Pb^*/^{238}U$	±%	err corr
GZ-28.1.1	0.46	130	120	0.95	6.6	367	4	297	130	−19	17.08	1.2	0.0523	5.7	0.42	5.8	0.0585	1.2	0.207
GZ-28.2.1	0.24	76	51	0.69	25.2	2087	19	2045	27	−2	2.61	1.1	0.1262	1.6	6.65	1.9	0.3822	1.1	0.561
GZ-28.3.1	0.00	238	82	0.36	16.4	496	4	555	48	12	12.50	0.9	0.0587	2.2	0.65	2.4	0.0800	0.9	0.363
GZ-28.4.1	0.34	173	49	0.29	11.6	482	5	444	84	−8	12.89	1.0	0.0558	3.8	0.60	3.9	0.0776	1.0	0.253
GZ-28.5.1	0.45	123	5	0.04	6.2	368	4	256	131	−31	17.00	1.2	0.0513	5.7	0.42	5.8	0.0588	1.2	0.206
GZ-28.6.1	0.53	150	42	0.29	10.4	498	5	474	117	−5	12.45	1.0	0.0566	5.3	0.63	5.4	0.0803	1.0	0.193
GZ-28.7.1	0.21	795	13	0.02	37.0	340	2	332	55	−2	18.48	0.7	0.0531	2.4	0.40	2.5	0.0541	0.7	0.262
GZ-28.8.1	0.28	706	273	0.40	32.0	330	2	308	62	−7	19.02	0.8	0.0525	2.7	0.38	2.8	0.0526	0.8	0.272
GZ-28.9.1	0.56	120	80	0.68	9.5	566	6	483	122	−15	10.89	1.1	0.0568	5.5	0.72	5.6	0.0918	1.1	0.193
GZ-28.10.1	0.17	227	65	0.30	15.5	492	4	403	54	−18	12.61	0.9	0.0548	2.4	0.60	2.6	0.0793	0.9	0.347
GZ-28.11.1	0.16	315	99	0.32	21.1	483	4	527	52	9	12.86	0.8	0.0579	2.4	0.62	2.5	0.0778	0.8	0.325
GZ-28.12.1	0.66	194	16	0.09	13.5	499	4	354	124	−29	12.42	0.9	0.0536	5.5	0.59	5.6	0.0805	0.9	0.159
GZ-28.13.1	0.60	87	33	0.39	6.2	509	6	439	143	−14	12.18	1.2	0.0557	6.4	0.63	6.5	0.0821	1.2	0.178
GZ-28.14.1	0.05	212	270	1.31	93.9	2678	15	2760	8	3	1.94	0.7	0.1921	0.5	13.64	0.8	0.5151	0.7	0.801
GZ-28.15.1	0.11	200	94	0.49	90.1	2717	16	2694	13	−1	1.91	0.7	0.1846	0.8	13.34	1.0	0.5243	0.7	0.687
GZ-28.16.1	-0.01	616	831	1.39	273.5	2685	14	2695	7	0	1.94	0.6	0.1847	0.4	13.15	0.8	0.5165	0.6	0.843

Errors are 1-sigma; Pb_c and Pb* indicate the common and radiogenic portions, respectively.
Error in Standard calibration was 0.4 % (not included in above errors but required when comparing data from different mounts).
(1) Common Pb corrected using measured ^{204}Pb.

Table S2 (continued): New U–Pb (SHRIMP) detrital zircon age data from the Carboniferous–Permian sedimentary formations of the Northern Gemericum. Note: the old zircon age data from the sample LA-66, taken from Vozárová et al. 2013, are shaded.

Rudňany Fm.

Spot	% $^{206}Pb_c$	ppm U	ppm Th	$^{232}Th/^{238}U$	ppm $^{206}Pb^*$	(1) $^{206}Pb/^{238}U$ Age		(1) $^{207}Pb/^{206}Pb$ Age		% Discordant	(1) $^{238}U/^{206}Pb^*$	±%	(1) $^{207}Pb^*/^{206}Pb^*$	±%	(1) $^{207}Pb^*/^{235}U$	±%	(1) $^{206}Pb^*/^{238}U$	±%	err corr
GZ-35_1.1	0.00	59	45	0.79	6.57	781.00	±13	832.00	±54	7	7.76	1.8	0.0668	2.6	1.19	3.2	0.1288	1.8	0.564
GZ-35_2.1	0.11	309	136	0.45	14.90	350.80	±5,2	354.00	±40	1	17.88	1.5	0.0536	1.8	0.41	2.3	0.0559	1.5	0.653
GZ-35_3.1	0.08	284	101	0.37	13.80	355.30	±5,3	364.00	±44	3	17.65	1.5	0.0538	2.0	0.42	2.5	0.0567	1.5	0.619
GZ-35_4.1	0.11	266	161	0.63	13.00	357.30	±5,4	371.00	±42	4	17.55	1.5	0.0540	1.9	0.42	2.4	0.0570	1.5	0.635
GZ-35_5.1	0.17	603	174	0.30	29.40	355.10	±5,2	347.00	±32	−2	17.66	1.5	0.0534	1.4	0.42	2.1	0.0566	1.5	0.725
GZ-35_6.1	0.10	250	472	1.95	23.60	671.70	±9,7	637.00	±30	−5	9.11	1.5	0.0609	1.4	0.92	2.1	0.1098	1.5	0.736
GZ-35_7.1	0.15	141	115	0.84	6.88	354.20	±5,6	340.00	±66	−4	17.70	1.6	0.0533	2.9	0.42	3.3	0.0565	1.6	0.482
GZ-35_8.1	0.07	365	3	0.01	104.00	1849.00	±24	2027.90	±8,2	10	3.01	1.5	0.1249	0.5	5.72	1.6	0.3322	1.5	0.955
GZ-35_9.1	0.06	446	169	0.39	200.00	2709.00	±33	2681.00	±15	−1	1.91	1.5	0.1831	0.9	13.19	1.7	0.5224	1.5	0.856
GZ-35_10.1	0.24	75	52	0.71	7.71	724.00	±12	698.00	±68	−4	8.41	1.7	0.0627	3.2	1.03	3.6	0.1189	1.7	0.467
GZ-35_11.1	0.01	249	252	1.04	130.00	3052.00	±37	2998.00	±16	−2	1.65	1.5	0.2224	1.0	18.57	1.8	0.6056	1.5	0.835
GZ-35_12.1	0.11	355	252	0.73	17.70	363.90	±5,4	330.00	±38	−9	17.22	1.5	0.0530	1.7	0.42	2.3	0.0581	1.5	0.672
GZ-35_13.1	0.06	175	54	0.32	74.60	2598.00	±32	2619.50	±8,3	1	2.01	1.5	0.1764	0.5	12.07	1.6	0.4963	1.5	0.949
GZ-35_14.1	0.03	761	224	0.30	237.00	1991.00	±25	2665.70	±9,7	34	2.76	1.5	0.1814	0.6	9.05	1.6	0.3618	1.5	0.927
GZ-35_15.1	0.04	724	248	0.35	38.20	384.10	±5,5	399.00	±24	4	16.29	1.5	0.0547	1.1	0.46	1.8	0.0614	1.5	0.805
GZ-35_16.1	0.26	166	44	0.27	11.50	497.10	±7,7	433.00	±64	−13	12.47	1.6	0.0555	2.9	0.61	3.3	0.0802	1.6	0.493

Errors are 1-sigma; Pb_c and Pb* indicate the common and radiogenic portions, respectively.
Error in Standard calibration was 0.51 %
(1) Common Pb corrected using measured ^{204}Pb.

Table S2 (continued): New U–Pb (SHRIMP) detrital zircon age data from the Carboniferous–Permian sedimentary formations of the Northern Gemericum. Note: the old zircon age data from the sample LA-66, taken from Vozárová et al. 2013, are shaded.

Rudňany Fm. – metasandstone pebble

Spot	% $^{206}Pb_c$	ppm U	ppm Th	$^{232}Th/^{238}U$	ppm $^{206}Pb^*$	(1) $^{206}Pb/^{238}U$ Age	±1s err	(1) $^{207}Pb/^{206}Pb$ Age	±1s err	% Discordant	(1) $^{238}U/^{206}Pb^*$	±%	(1) $^{207}Pb^*/^{206}Pb^*$	±%	(1) $^{207}Pb^*/^{235}U$	±%	(1) $^{206}Pb^*/^{238}U$	±%	err corr
GZ-36A.1.1	0.06	233	92	0.41	96.1	2529	16	2561	11	1	2.08	0.8	0.1703	0.7	11.28	1.0	0.4805	0.8	0.757
GZ-36A.2.1	0.13	66	27	0.43	20.8	2022	21	2034	31	1	2.71	1.2	0.1254	1.8	6.37	2.2	0.3684	1.2	0.563
GZ-36A.3.1	0.08	62	23	0.38	31.8	3000	36	2941	22	−2	1.69	1.5	0.2147	1.4	17.54	2.0	0.5925	1.5	0.735
GZ-36A.4.1	0.19	201	16	0.08	62.8	1996	14	2007	18	1	2.75	0.8	0.1235	1.0	6.18	1.3	0.3629	0.8	0.615
GZ-36A.5.1	0.37	66	36	0.56	22.2	2119	23	2060	32	−3	2.57	1.3	0.1272	1.8	6.83	2.2	0.3891	1.3	0.573
GZ-36A.6.1	0.15	294	120	0.42	90.3	1965	13	2025	14	3	2.80	0.8	0.1248	0.8	6.13	1.1	0.3564	0.8	0.708
GZ-36A.7.1	0.03	402	236	0.61	181.4	2720	14	2706	7	−1	1.90	0.6	0.1858	0.4	13.45	0.8	0.5250	0.6	0.832
GZ-36A.8.1	0.12	85	17	0.21	28.0	2082	22	2013	35	−3	2.62	1.3	0.1239	2.0	6.51	2.3	0.3811	1.3	0.537
GZ-36A.9.1	0.46	157	214	1.41	12.7	576	5	569	83	−1	10.70	1.0	0.0591	3.8	0.76	3.9	0.0934	1.0	0.245
GZ-36A.10.1	0.14	144	88	0.63	41.8	1874	13	1882	28	0	2.96	0.8	0.1151	1.5	5.36	1.7	0.3375	0.8	0.464
GZ-36A.11.1	0.12	194	56	0.30	87.6	2718	16	2706	10	0	1.91	0.7	0.1859	0.6	13.44	0.9	0.5244	0.7	0.747
GZ-36A.12.1	0.27	105	74	0.73	7.9	537	6	489	92	−9	11.50	1.1	0.0569	4.2	0.68	4.3	0.0869	1.1	0.249
GZ-36A.13.1	0.07	316	55	0.18	141.5	2700	14	2737	14	1	1.92	0.6	0.1894	0.8	13.58	1.0	0.5201	0.6	0.591
GZ-36A.14.1	0.04	170	207	1.25	73.6	2626	17	2770	11	5	1.99	0.8	0.1932	0.7	13.39	1.0	0.5027	0.8	0.765
GZ-36A.15.1	0.06	214	92	0.44	72.2	2134	12	2136	13	0	2.55	0.7	0.1328	0.8	7.19	1.0	0.3923	0.7	0.659
GZ-36A.16.1	-0.01	626	106	0.17	280.4	2705	13	2688	5	−1	1.92	0.6	0.1838	0.3	13.21	0.7	0.5213	0.6	0.891
GZ-36A.17.1	0.12	210	70	0.34	87.3	2543	14	2514	24	−1	2.07	0.7	0.1657	1.4	11.05	1.6	0.4837	0.7	0.426
GZ-36A.18.1	-0.01	836	164	0.20	361.7	2630	19	2834	20	8	1.99	0.9	0.2010	1.2	13.96	1.5	0.5037	0.9	0.592

Errors are 1-sigma; Pb_c and Pb* indicate the common and radiogenic portions, respectively.
Error in Standard calibration was 0.4 % (not included in above errors but required when comparing data from different mounts).
(1) Common Pb corrected using measured ^{204}Pb.

Table S2 (continued): New U–Pb (SHRIMP) detrital zircon age data from the Carboniferous–Permian sedimentary formations of the Northern Gemericum. Note: the old zircon age data from the sample LA-66, taken from Vozárová et al. 2013, are shaded.

Rudňany Fm. – gneiss pebble

Spot	% $^{206}Pb_c$	ppm U	ppm Th	$^{232}Th/^{238}U$	ppm $^{206}Pb^*$	(1) $^{206}Pb/^{238}U$ Age		(1) $^{207}Pb/^{206}Pb$ Age		% Discordant	(1) $^{238}U/^{206}Pb^*$	±%	(1) $^{207}Pb^*/^{206}Pb^*$	±%	(1) $^{207}Pb^*/^{235}U$	±%	(1) $^{206}Pb^*/^{238}U$	±%	err corr
GZ55_1.1	0.23	383	89	0.24	28.50	534.20	±2,5	552.00	±37	3	11.57	0.49	0.0586	1.70	0.70	1.80	0.0864	0.49	0.276
GZ55_1.2	1.48	68	4	0.06	3.65	385.70	±6,3	530.00	±400	37	16.21	1.70	0.0580	18.00	0.49	18.00	0.0617	1.70	0.093
GZ55_2.1	0.25	271	26	0.10	18.50	491.60	±3,8	456.00	±46	−7	12.62	0.80	0.0561	2.10	0.61	2.20	0.0792	0.80	0.358
GZ55_3.1	0.12	710	137	0.20	50.70	513.70	±1,9	517.00	±43	1	12.06	0.38	0.0577	2.00	0.66	2.00	0.0829	0.38	0.191
GZ55_4.1	0.17	460	87	0.20	33.30	521.00	±2,3	486.00	±36	−7	11.88	0.47	0.0569	1.60	0.66	1.70	0.0842	0.47	0.278
GZ55_5.1	0.08	1332	346	0.27	94.20	509.60	±1,5	512.00	±18	0	12.16	0.31	0.0575	0.80	0.65	0.86	0.0823	0.31	0.358
GZ55_6.1	0.12	1084	81	0.08	75.90	504.40	±1,6	510.00	±20	1	12.29	0.33	0.0575	0.92	0.65	0.98	0.0814	0.33	0.339
GZ55_6.2	0.77	71	0	0.01	3.82	386.70	±4,9	464.00	±130	20	16.17	1.30	0.0563	5.80	0.48	5.90	0.0618	1.30	0.221
GZ55_7.1	0.03	1840	695	0.39	132.00	518.00	±1,4	538.00	±13	4	11.95	0.28	0.0582	0.60	0.67	0.66	0.0837	0.28	0.424
GZ55_8.1	0.08	1352	442	0.34	98.30	523.40	±2,3	516.00	±19	−1	11.82	0.46	0.0576	0.87	0.67	0.99	0.0846	0.46	0.467

Errors are 1-sigma; Pb_c and Pb* indicate the common and radiogenic portions, respectively.
Error in Standard calibration was 0.36 % (not included in above errors but required when comparing data from different mounts).
(1) Common Pb corrected using measured ^{204}Pb.

Table S2 (continued): New U–Pb (SHRIMP) detrital zircon age data from the Carboniferous–Permian sedimentary formations of the Northern Gemericum. Note: the old zircon age data from the sample LA-66, taken from Vozárová et al. 2013, are shaded.

Hámor Fm.

Spot	% $^{206}Pb_c$	ppm U	ppm Th	$^{232}Th/^{238}U$	ppm $^{206}Pb^*$	(1) $^{206}Pb/^{238}U$ Age		(2) $^{206}Pb/^{238}U$ Age		(3) $^{206}Pb/^{238}U$ Age		(1) $^{207}Pb/^{206}Pb$ Age		% Discordant	Total $^{238}U/^{206}Pb$	±%	Total $^{207}Pb/^{206}Pb$	±%	(1) $^{238}U/^{206}Pb^*$	±%	(1) $^{207}Pb^*/^{206}Pb^*$	±%	(1) $^{207}Pb^*/^{235}U$	±%	(1) $^{206}Pb^*/^{238}U$	±%	err corr
29LA.1.1	0.23	308	337	1.13	24.0	558.4	±9,2	559.2	±9,4	560.0	±11	516	±36	−8	11.03	1.70	0.0595	1.20	11.05	1.70	0.0577	1.60	0.72	2.40	0.0905	1.70	0.727
29LA.2.1	0.26	508	187	0.38	24.1	346.2	±5,8	346.8	±5,9	346.3	6.30	287	±49	−17	18.08	1.70	0.0542	1.50	18.13	1.70	0.0520	2.20	0.40	2.80	0.0552	1.70	0.625
29LA.3.1	0.26	667	161	0.25	46.0	496.8	±8,1	497.9	±8,3	497.6	±8,5	421	±37	−15	12.45	1.70	0.0573	0.99	12.48	1.70	0.0552	1.60	0.61	2.40	0.0801	1.70	0.719
29LA.4.1	0.23	914	228	0.26	44.2	352.0	±5,8	352.9	±5,9	352.9	±6,1	265	±32	−25	17.78	1.70	0.0534	1.10	17.82	1.70	0.0515	1.40	0.40	2.20	0.0561	1.70	0.775
29LA.5.1	0.92	109	45	0.43	13.2	843.0	±17	847.0	±18	851.0	±18	721	±66	−14	7.09	2.10	0.0711	1.50	7.15	2.10	0.0634	3.10	1.22	3.80	0.1397	2.10	0.570
29LA.6.1	0.14	1500	792	0.55	96.5	464.7	±7,5	465.3	±7,6	466.6	±8,2	423	±18	−9	13.36	1.70	0.0565	0.60	13.38	1.70	0.0553	0.81	0.57	1.90	0.0747	1.70	0.899
29LA.7.1	0.47	220	112	0.52	18.4	595.1	± 9,9	597.0	±10	599.0	±11	513	±48	−14	10.29	1.70	0.0614	1.30	10.34	1.70	0.0576	2.20	0.77	2.80	0.0967	1.70	0.624
29LA.8.1	1.07	156	90	0.60	13.3	607.0	±10	611.0	±11	613.0	±11	410	±84	−32	10.02	1.80	0.0638	1.50	10.13	1.80	0.0549	3.80	0.75	4.20	0.0987	1.80	0.427
29LA.9.1	0.10	346	121	0.36	21.7	453.0	±7,6	452.6	±7,7	454.3	±8,1	481	±43	6	13.72	1.70	0.0576	1.60	13.74	1.70	0.0567	2.00	0.57	2.60	0.0728	1.70	0.665
29LA.10.1	0.21	866	374	0.45	67.7	560.3	±9	560.4	±9,2	559.5	±9,7	556	±22	−1	10.99	1.70	0.0604	0.82	11.01	1.70	0.0587	1.00	0.74	2.00	0.0908	1.70	0.856
29LA.11.1	0.15	746	366	0.51	56.6	544.7	±8,8	545.0	±9	544.6	±9,5	531	±24	−2	11.32	1.70	0.0593	0.91	11.34	1.70	0.0580	1.10	0.71	2.00	0.0882	1.70	0.839
29LA.12.1	0.84	80	58	0.75	6.5	577.0	±11	581.0	±11	576.0	±12	397	±120	−31	10.58	1.90	0.0615	2.60	10.67	1.90	0.0546	5.10	0.71	5.50	0.0937	1.90	0.353
29LA.13.1	0.09	862	545	0.65	73.2	607.0	±10	607.0	±10	607.0	±11	622	±20	3	10.12	1.70	0.0612	0.79	10.13	1.70	0.0605	0.91	0.82	2.00	0.0987	1.70	0.887
29LA.14.1	0.28	173	175	1.04	52.1	1 928.0	±29	1 904.0	±33	1 925.0	±34	2 095	±13	9	2.86	1.80	0.1322	0.66	2.87	1.80	0.1298	0.76	6.24	1.90	0.3486	1.80	0.917
29LA.15.1	0.31	334	104	0.32	42.0	878.0	±14	878.0	±15	879.0	±15	891	±33	1	6.83	1.70	0.0713	0.99	6.85	1.70	0.0687	1.60	1.38	2.40	0.1460	1.70	0.729
29LA.16.1	1.14	60	17	0.29	10.8	1 203.0	±21	1 201.0	±22	1 210.0	±22	1 269	±71	5	4.81	1.90	0.0926	2.30	4.87	1.90	0.0830	3.60	2.35	4.10	0.2052	1.90	0.469
29LA.16.2	0.19	1286	28	0.02	84.7	475.2	±7,9	475.7	±8	475.8	±7,9	441	±21	−7	13.05	1.70	0.0572	0.76	13.07	1.70	0.0557	0.94	0.59	2.00	0.0765	1.70	0.878
29LA.17.1	0.61	45	45	1.04	3.9	622.0	±14	622.0	±14	633.0	±17	600	±130	−3	9.82	2.30	0.0649	3.30	9.88	2.30	0.0599	6.00	0.84	6.40	0.1012	2.30	0.357
29LA.18.1	0.19	870	313	0.37	45.8	383.0	6.30	383.7	±6,4	383.9	±6,7	316	±34	−17	16.31	1.70	0.0543	1.00	16.34	1.70	0.0527	1.50	0.45	2.30	0.0612	1.70	0.745
29LA.18.2	0.78	167	48	0.29	8.4	365.0	6.60	366.6	±6,6	364.6	±7	206	±120	−44	17.03	1.80	0.0566	2.50	17.17	1.90	0.0502	5.10	0.40	5.40	0.0583	1.90	0.342
29LA.19.1	0.07	234	139	0.62	74.3	2 030.0	±30	2 002.0	±34	2 032.0	±32	2 195	±10	8	2.70	1.70	0.1380	0.55	2.70	1.70	0.1374	0.58	7.01	1.80	0.3702	1.70	0.948
29LA.20.1	0.03	1065	861	0.84	87.5	588.7	±9,4	588.4	±9,6	590.0	±11	606	±17	3	10.45	1.70	0.0603	0.71	10.46	1.70	0.0601	0.80	0.79	1.90	0.0956	1.70	0.903
29LA.21.1	0.11	843	1686	2.07	67.2	571.4	±9,2	571.8	±9,4	580.0	±14	549	±23	−4	10.78	1.70	0.0594	0.83	10.79	1.70	0.0585	1.10	0.75	2.00	0.0927	1.70	0.847
29LA.22.1	0.56	272	187	0.71	22.4	586.0	±10	588.0	±11	591.0	±12	472	±55	−19	10.45	1.90	0.0611	1.40	10.51	1.90	0.0565	2.50	0.74	3.10	0.0951	1.90	0.600
29LA.23.1	0.50	210	81	0.40	21.5	724.0	±13	725.0	±13	710.0	±14	676	±47	−7	8.37	1.90	0.0662	1.40	8.42	1.90	0.0621	2.20	1.02	2.90	0.1188	1.90	0.648

Errors are 1-sigma; Pb_c and Pb* indicate the common and radiogenic portions, respectively.
(1) Common Pb corrected using measured ^{204}Pb.
(2) Common Pb corrected by assuming $^{206}Pb/^{238}U$–$^{207}Pb/^{235}U$ age-concordance
(3) Common Pb corrected by assuming $^{206}Pb/^{238}U$–$^{208}Pb/^{232}Th$ age-concordance

Table S2 (continued): New U–Pb (SHRIMP) detrital zircon age data from the Carboniferous–Permian sedimentary formations of the Northern Gemericum. Note: the old zircon age data from the sample LA-66, taken from Vozárová et al. 2013, are shaded.

Hámor Fm.

Spot	% $^{206}Pb_c$	ppm U	ppm Th	$^{232}Th/^{238}U$	ppm $^{206}Pb^*$	(1) $^{206}Pb/^{238}U$ Age	±1s err	(1) $^{207}Pb/^{206}Pb$ Age	±1s err	% Discordant	(1) $^{238}U/^{206}Pb^*$	±%	(1) $^{207}Pb^*/^{206}Pb^*$	±%	(1) $^{207}Pb/^{235}U$	±%	(1) $^{206}Pb^*/^{238}U$	±%	err corr
GZ-27.1.1	1.00	96	113	1.22	7.0	522	9	667	207	28	11.85	1.8	0.0618	9.7	0.72	9.8	0.0844	1.8	0.180
GZ-27.2.1	0.20	74	125	1.74	24.4	2077	20	2107	29	1	2.63	1.1	0.1307	1.7	6.85	2.0	0.3801	1.1	0.558
GZ-27.3.1	-0.11	137	133	1.00	58.7	2608	22	2832	26	9	2.01	1.0	0.2007	1.6	13.80	1.9	0.4987	1.0	0.550
GZ-27.4.1	0.06	112	96	0.88	54.4	2886	23	2936	13	2	1.77	1.0	0.2140	0.8	16.66	1.3	0.5647	1.0	0.770
GZ-27.5.1	-0.01	228	57	0.26	80.9	2232	15	2396	32	7	2.42	0.8	0.1544	1.9	8.81	2.1	0.4138	0.8	0.392
GZ-27.6.1	0.27	49	38	0.82	16.1	2101	24	2066	38	−2	2.59	1.4	0.1276	2.2	6.78	2.6	0.3854	1.4	0.532
GZ-27.7.1	0.03	437	126	0.30	172.2	2435	14	2552	15	5	2.18	0.7	0.1694	0.9	10.72	1.1	0.4589	0.7	0.609
GZ-27.8.1	0.03	1318	191	0.15	494.1	2334	12	2451	6	5	2.29	0.6	0.1596	0.4	9.60	0.7	0.4363	0.6	0.869
GZ-27.9.1	0.09	1501	408	0.28	63.4	309	2	278	46	−10	20.36	0.7	0.0518	2.0	0.35	2.1	0.0491	0.7	0.343
GZ-27.10.1	0.00	542	285	0.54	237.3	2654	14	2681	15	1	1.96	0.7	0.1831	0.9	12.86	1.1	0.5094	0.7	0.589
GZ-27.11.1	0.15	428	252	0.61	29.5	497	4	433	52	−13	12.47	0.8	0.0555	2.3	0.61	2.4	0.0802	0.8	0.319
GZ-27.12.1	0.15	126	104	0.85	10.2	577	6	587	78	2	10.68	1.1	0.0595	3.6	0.77	3.8	0.0936	1.1	0.296
GZ-27.13.1	0.02	1146	943	0.85	48.2	308	2	236	34	−23	20.44	0.7	0.0509	1.5	0.34	1.6	0.0489	0.7	0.410
GZ-27.14.1	0.07	101	45	0.46	45.0	2689	21	2709	15	1	1.93	1.0	0.1862	0.9	13.29	1.3	0.5177	1.0	0.718
GZ-27.15.1	0.32	134	215	1.66	8.5	460	5	476	124	3	13.50	1.2	0.0566	5.6	0.58	5.7	0.0740	1.2	0.204
GZ-27.16.1	0.09	605	538	0.92	42.3	504	3	467	35	−7	12.30	0.7	0.0564	1.6	0.63	1.7	0.0813	0.7	0.394

Errors are 1-sigma; Pb_c and Pb* indicate the common and radiogenic portions, respectively.
Error in Standard calibration was 0.4 % (not included in above errors but required when comparing data from different mounts).
(1) Common Pb corrected using measured ^{204}Pb.

Table S2 (continued): New U–Pb (SHRIMP) detrital zircon age data from the Carboniferous–Permian sedimentary formations of the Northern Gemericum. Note: the old zircon age data from the sample LA-66, taken from Vozárová et al. 2013, are shaded.

Petrova Hora Fm.

Spot	% $^{206}Pb_c$	ppm U	ppm Th	$^{232}Th/^{238}U$	ppm $^{206}Pb^*$	(1) $^{206}Pb/^{238}U$ Age		(2) $^{206}Pb/^{238}U$ Age		(1) $^{207}Pb/^{206}Pb$ Age		% Discordant	Total $^{238}U/^{206}Pb$	±%	Total $^{207}Pb/^{206}Pb$	±%	(1) $^{238}U^{206}Pb^*$	±%	(1) $^{207}Pb^*/^{206}Pb^*$	±%	(1) $^{207}Pb^*/^{235}U$	±%	(1) $^{206}Pb^*/^{238}U$	±%	err corr
74LA_1.1	0.00	139	67	0.49	50.6	2270.0	±45	2280.0	±55	2222	±12	−2	2.37	2.30	0.1396	0.71	2.37	2.3	0.1396	0.71	8.12	2.40	0.4220	2.30	0.956
74LA_2.1	0.06	708	65	0.09	43.9	448.9	±8,4	449.0	±8,5	437	±23	−3	13.86	1.90	0.0561	0.93	13.87	1.9	0.0556	1.00	0.55	2.20	0.0721	1.90	0.885
74LA_3.1	0.09	646	379	0.61	32.7	368.1	±6,9	368.1	±7	365	±31	−1	17.00	1.90	0.0546	1.10	17.02	1.9	0.0539	1.40	0.44	2.40	0.0588	1.90	0.818
74LA_4.1	0.00	421	163	0.40	54.3	901.0	±16	902.0	±17	885	±16	−2	6.67	1.90	0.0685	0.77	6.67	1.9	0.0685	0.77	1.42	2.10	0.1500	1.90	0.929
74LA_5.1	0.12	2422	858	0.37	116.0	350.3	±6,5	350.5	±6,6	327	±23	−7	17.89	1.90	0.0540	0.90	17.91	1.9	0.0530	1.00	0.41	2.20	0.0558	1.90	0.881
74LA_6.1	0.24	500	68	0.14	24.2	352.5	±6,7	352.5	±6,8	356	±43	1	17.75	1.90	0.0556	1.40	17.79	2.0	0.0536	1.90	0.42	2.70	0.0562	2.00	0.713
74LA_7.1	0.05	214	99	0.48	14.6	493.1	±9,4	493.2	±9,6	489	±37	−1	12.57	2.00	0.0573	1.60	12.58	2.0	0.0569	1.70	0.62	2.60	0.0795	2.00	0.766
74LA_8.1	0.51	15	6	0.42	2.6	1201.0	±31	1200.0	±33	1215	±140	1	4.86	2.80	0.0850	5.70	4.88	2.8	0.0807	7.00	2.28	7.60	0.2048	2.80	0.376
74LA_9.1	0.58	129	1	0.01	7.8	433.2	±8,6	433.5	±8,7	408	±83	−6	14.30	2.00	0.0596	2.10	14.39	2.0	0.0549	3.70	0.53	4.20	0.0695	2.00	0.486
74LA_10.1	0.07	427	143	0.34	17.4	298.4	±5,7	298.4	±5,8	291	±45	−2	21.09	2.00	0.0527	1.70	21.11	2.0	0.0521	2.00	0.34	2.80	0.0474	2.00	0.708
74LA_11.1	0.12	611	389	0.66	39.2	464.0	±8,7	464.2	±8,8	452	±29	−3	13.38	1.90	0.0570	1.10	13.40	1.9	0.0560	1.30	0.58	2.30	0.0746	1.90	0.824
74LA_12.1	0.21	125	63	0.52	7.9	455.8	±9,1	455.8	±9,3	459	±65	1	13.62	2.10	0.0578	2.50	13.65	2.1	0.0562	2.90	0.57	3.60	0.0733	2.10	0.578
74LA_13.1	0.11	512	147	0.30	21.2	303.4	±5,8	303.4	±5,9	301	±40	−1	20.73	2.00	0.0533	1.60	20.75	2.0	0.0524	1.80	0.35	2.60	0.0482	2.00	0.744
74LA_14.1	0.02	587	228	0.40	35.1	433.9	±8,2	434.2	±8,3	408	±28	−6	14.36	1.90	0.0551	1.20	14.36	1.9	0.0549	1.20	0.53	2.30	0.0696	1.90	0.845
74LA_15.1	0.37	116	121	1.08	15.4	923.0	±17	924.0	±18	910	±44	−1	6.47	2.00	0.0725	1.60	6.49	2.0	0.0694	2.20	1.47	3.00	0.1540	2.00	0.686
74LA_16.1	0.11	653	433	0.69	31.0	346.4	±6,6	346.5	±6,6	345	±32	0	18.09	1.90	0.0543	1.30	18.11	1.9	0.0534	1.40	0.41	2.40	0.0552	1.90	0.808
74LA_17.1	0.09	597	172	0.30	31.1	379.4	±7,2	379.4	±7,2	382	±38	1	16.48	1.90	0.0550	1.50	16.49	1.9	0.0543	1.70	0.45	2.60	0.0606	1.90	0.751

Errors are 1-sigma; Pb_c and Pb* indicate the common and radiogenic portions, respectively.
Error in Standard calibration was 0.5 % (not included in above errors but required when comparing data from different mounts).
(1) Common Pb corrected using measured ^{204}Pb.
(2) Common Pb corrected by assuming $^{206}Pb/^{238}U$–$^{207}Pb/^{235}U$ age-concordance

Table S2 (continued): New U–Pb (SHRIMP) detrital zircon age data from the Carboniferous–Permian sedimentary formations of the Northern Gemericum. Note: the old zircon age data from the sample LA-66, taken from Vozárová et al. 2013, are shaded.

Novoveská Huta Fm. – new and older, recalculated, published data (gray)

Spot	% $^{206}Pb_c$	ppm U	ppm Th	$^{232}Th/^{238}U$	ppm $^{206}Pb^*$	(1) $^{206}Pb/^{238}U$ Age		(1) $^{207}Pb/^{206}Pb$ Age		% Discordant	(1) $^{207}Pb^*/^{206}Pb^*$	±%	(1) $^{207}Pb^*/^{235}U$	±%	(1) $^{206}Pb^*/^{238}U$	±%	err corr
66LA_1.1	0.28	526	178	0.35	22.0	305.9	±6,1	251.0	±63	−18	0.0512	2.70	0.34	3.4	0.0486	2.0	0.595
66LA_2.1	0.04	798	186	0.24	32.8	301.1	±5,9	279.0	±40	−7	0.0518	1.80	0.34	2.7	0.0478	2.0	0.754
66LA_3.1	0.69	339	186	0.57	13.0	279.5	±5,8	128.0	±140	−54	0.0486	5.80	0.30	6.2	0.0443	2.1	0.340
66LA_4.1	0.11	348	173	0.51	13.3	280.6	±5,9	285.0	±77	2	0.0520	3.40	0.32	4.0	0.0445	2.2	0.540
66LA_5.1	0.74	174	17	0.10	8.7	361.1	±7,7	230.0	±140	−36	0.0508	5.90	0.40	6.3	0.0576	2.2	0.348
66LA_6.1	0.08	478	194	0.42	24.0	366.0	±7,4	320.0	±52	−13	0.0528	2.30	0.43	3.1	0.0584	2.1	0.670
66LA_7.1	0.09	1865	447	0.25	97.2	379.3	±7,4	394.0	±26	4	0.0546	1.20	0.46	2.3	0.0606	2.0	0.866
66LA_8.1	0.09	450	315	0.72	36.9	588.0	±12	541.0	±36	−8	0.0583	1.60	0.77	2.6	0.0955	2.0	0.784
66LA_9.1	0.00	646	295	0.47	26.5	301.1	±6,1	304.0	±41	1	0.0524	1.80	0.35	2.7	0.0478	2.1	0.750
66LA_10.1	–	610	136	0.23	312.0	3012.0	±49	2725.0	±15	−10	0.1881	0.91	15.44	2.2	0.5950	2.1	0.914
66LA_11.1	0.01	261	68	0.27	120.0	2760.0	±52	2697.3	± 9,9	−2	0.1849	0.60	13.62	2.4	0.5340	2.3	0.969
66LA_12.1	0.06	180	106	0.61	60.4	2130.0	±39	2314.0	±22	9	0.1472	1.30	7.95	2.5	0.3916	2.1	0.859
66LA_13.1	0.37	435	58	0.14	27.6	458.0	±9,2	457.0	±78	0	0.0561	3.50	0.57	4.1	0.0736	2.1	0.509
66LA_14.1	0.36	612	235	0.40	24.8	296.1	±6	160.0	±100	−46	0.0492	4.30	0.32	4.8	0.0470	2.1	0.431
66LA_15.1	0.21	461	135	0.30	19.0	301.9	±6,2	254.0	±92	−16	0.0513	4.00	0.34	4.5	0.0480	2.1	0.466
66LA_16.1	0.00	227	115	0.52	9.2	295.3	±6,3	240.0	±88	−19	0.0510	3.80	0.33	4.4	0.0469	2.2	0.496
66LA_17.1	0.06	554	343	0.64	28.1	369.8	±7,4	377.0	±57	2	0.0541	2.60	0.44	3.3	0.0590	2.1	0.630
66LA_17.2	–	835	225	0.28	42.8	374.3	±8,4	419.0	±50	12	0.0552	2.20	0.46	3.2	0.0598	2.3	0.718
66LA_18.1	–	217	235	1.12	10.8	363.7	±7,9	411.0	±69	13	0.0550	3.10	0.44	3.8	0.0580	2.2	0.587
66LA_19.1	0.18	616	237	0.40	31.1	367.3	±7,5	413.0	±56	13	0.0550	2.50	0.45	3.3	0.0586	2.1	0.638
66LA_20.1	0.23	614	45	0.08	40.1	471.3	±9,7	480.0	46.00	2	0.0567	2.10	0.59	3.0	0.0759	2.1	0.716
66LA_21.1	0.50	378	186	0.51	18.5	356.1	±7,8	382.0	±100	7	0.0543	4.60	0.43	5.2	0.0568	2.2	0.435
66LA_22.1	0.16	596	350	0.61	22.4	275.8	±5,9	227.0	±80	−18	0.0507	3.50	0.31	4.1	0.0437	2.2	0.536
66LA_24.1	0.06	1696	32	0.02	83.0	356.8	±6,7	346.0	±21	−3	0.0534	0.91	0.42	2.1	0.0569	1.9	0.903
66LA_25.1	0.25	121	72	0.62	38.6	2023.0	±35	2090.0	±15	3	0.1294	0.86	6.58	2.2	0.3686	2.0	0.921
66LA_26.1	0.03	806	561	0.72	38.9	352.7	±6,6	335.0	±28	−5	0.0532	1.20	0.41	2.3	0.0562	1.9	0.846
66LA_27.1	0.00	443	332	0.77	21.9	360.2	±6,9	333.0	±36	−7	0.0531	1.60	0.42	2.5	0.0575	2.0	0.778
66LA_28.1	0.12	424	9	0.02	28.3	480.8	±9	452.0	±36	−6	0.0560	1.60	0.60	2.5	0.0774	2.0	0.773
66LA_29.1	0.16	110	56	0.53	7.8	513.0	±10	474.0	±66	−7	0.0566	3.00	0.65	3.6	0.0828	2.1	0.572
66LA_30.1	0.27	400	80	0.21	27.5	495.3	±9,3	473.0	±42	−4	0.0565	1.90	0.62	2.7	0.0799	2.0	0.718
66LA_31.1	0.04	713	170	0.25	156.0	1462.0	±25	1502.2	±9,8	3	0.0937	0.52	3.29	2.0	0.2546	1.9	0.966
66LA_32.1	0.02	681	710	1.08	290.0	2598.0	±48	2653.2	±4,2	2	0.1800	0.25	12.32	2.3	0.4960	2.2	0.994
66LA_33.1	0.02	561	143	0.26	38.3	493.6	±9,2	485.0	±26	−2	0.0568	1.20	0.62	2.3	0.0796	1.9	0.854

Errors are 1-sigma; Pb_c and Pb* indicate the common and radiogenic portions, respectively.
Error in Standard calibration was 0.64 %
(1) Common Pb corrected using measured ^{204}Pb.